8-28-2023 2:00 PM

Parametric Analysis and Enhancement of the Burst Capacity Model for Composite-Repaired Corroded Pipelines

Rodrigo Silva Silva-Santisteban, *Western University*

Supervisor: Zhou, Wenxing, *The University of Western Ontario*

A thesis submitted in partial fulfillment of the requirements for the Master of Engineering Science degree in Civil and Environmental Engineering

Abstract

One of the main causes of pipeline failures is corrosion, which leads to a localized loss of the pipe wall thickness and hence compromises the capacity of the pipeline. Composite repair is a method to rehabilitate corroded pipelines. Design codes such as ASME PCC-2 are commonly used to design the repair thickness. As the predictive accuracy to determine the burst capacity of a composite repaired pipeline with existing models is generally poor, the main objective of the present thesis is to provide insights on the parameters that affect the burst capacity and propose improvements to the prediction of burst capacity of composite repaired corroded pipelines.

The first study investigates the influence of defect width on the burst capacity of corroded pipelines repaired with composite materials. Parametric finite element analysis is conducted to assess the burst capacities of composite-repaired corroded pipelines containing localized and full-circumferential corrosion defects. The analysis reveals that composite-repaired pipes with localized defects exhibit considerably lower burst capacities compared to those with full-circumferential defects. Furthermore, the burst capacity model derived from the ASME PCC-2 code´s design equation is deemed non-conservative for composite-repaired pipes with localized defects based on the parametric finite element analyses. To address this issue, an empirical equation for the defect width correction factor is developed, demonstrating its high effectiveness in enhancing the predictive accuracy of the PCC-2 burst capacity model.

The second study addresses the limitations of existing prediction models that fail to account for the complexities of composite materials and the impact of defect dimensions on the burst capacity of composite-repaired corroded pipelines. An improved equation is proposed to enhance the ASME PCC-2 design code's ability to predict the burst capacity of such pipelines by incorporating a correction term into the model. To determine the correction term, a machine learning model called Gaussian process regression (GPR) is employed, utilizing seven input variables. The finite element parametric analysis data is divided into a training set (70%) and a test set (30%) using a stratified random approach to ensure equal representation of failure modes in both sets. The GPR model is constructed using a squared exponential kernel and a zero-mean function based on the training set data. The performance of the model is then

evaluated using the test set. Results indicate that the proposed model accurately predicts the burst pressure of the validation set with a mean absolute error of 4.0%. In comparison, the mean absolute error for the ASME PCC-2 model was 48%, demonstrating a significant improvement in accuracy.

Keywords

Corroded pipeline; Burst Capacity; Composite repair; Finite element analysis; Gaussian Process Regression

Summary for Lay Audience

Pipeline failures often occur due to corrosion, which weakens the pipe and reduces its capacity. Composite repair is a method used to fix corroded pipelines. However, current models for predicting the strength of repaired pipelines are not very accurate. This thesis aims to improve the prediction of burst capacity (maximum pressure it can withstand) for composite-repaired corroded pipelines.

The first study focuses on the width of the corrosion defect. It is found that pipes with localized defects repaired using composites have lower burst capacities compared to those with full-circumferential defects. The existing design equation from the ASME PCC-2 code is found to be unreliable for localized defects. To address this, a new equation is developed, correcting for the defect width and significantly improving the accuracy of burst capacity prediction.

The second study addresses the limitations of existing prediction models that don't consider the complexities of composite materials and the impact of defect dimensions. An improved equation is proposed by incorporating a correction term into the ASME PCC-2 model. To determine this correction term, a machine learning model called Gaussian process regression (GPR) is used. The GPR model is trained using data from finite element analysis and seven input variables. The model's performance is evaluated, and the results show that it accurately predicts the burst pressure of the pipeline with a small error of 4.0%. In contrast, the ASME PCC-2 model has a much larger error of 48%, indicating a significant improvement in accuracy with the proposed model.

Co-Authorship Statement

A shorter version of chapter 2 co-authored by Dr. Wenxing Zhou has been accepted as a technical paper and presented in the *Pressure Vessels and Piping Conference* (PVP 2023) in Atlanta, Georgia between July 17 and July 21, 2023.

Chapter 2 co-authored by Dr. Wenxing. Zhou has been submitted to the *Journal of Pressure Vessel Technology* as a technical paper.

Chapter 3 co-authored by Dr. Wenxing. Zhou is being prepared as a technical paper and will be submitted to the *Journal of Pressure Vessel Technology*.

Acknowledgments

To my beloved wife. Your patience, understanding and countless sacrifices have continually propelled me towards greater heights. Thank you for always being there and your unconditional, endless support. I am eternally grateful to have you by my side.

I would like to express my deepest gratitude to my family, whose love and support have been the foundation of my journey. Their unwavering belief in me has been a constant source of inspiration, and I am forever indebted to them for their presence in my life.

Finally, I am profoundly grateful to my supervisor Wenxing Zhou, for his guidance, expertise, and invaluable support throughout the entire research journey.

Table of Contents

List of Tables

List of Figures

Chapter 1

1 Introduction

1.1 Background

Buried steel oil and gas pipelines are vital components of the critical infrastructure systems in modern societies, spanning thousands of kilometers. However, many pipelines worldwide, including those in Canada, are aging and experiencing degradation over time. One significant degradation mechanism is corrosion, which causes localized thinning of the pipe wall and compromises the pipeline's ability to withstand high operating pressures.

To address the damage and degradations in pipelines, composite repair is a widely used method. It involves applying a composite material to the affected section of the pipe. The composite material bonds with the pipe surface, creating a strong protective layer that reinforces the pipe and restores its structural integrity. This repair process typically involves laying pre-impregnated sheets of glass or carbon fiber on the pipe's exterior and curing them on-site. Composite repair is cost-effective, efficient, and durable, as the composite material is resistant to corrosion, abrasion, and other forms of wear and tear [1].

Composite repairs consist of three basic components: the substrate, putty and fibre reinforced polymer (FRP). The substrate is the surface to which the composite repair will be applied (i.e. the corroded steel pipeline section); the putty is a filler material used to create a smooth surface on top of the substrate, and FRP is the composite material used to repair the damaged pipe. The basic design approach of composite-repaired corroded (CRC) pipelines is that the hoop stress in the defect area is mechanically transferred from the substrate to the FRP sleeve. Results from [2,3] indicate that up to substrate yielding, the substrate carries most of the hoop stress due to the steel high elastic’s modulus. After yielding, the composite reinforcements starts to carry a more substantial part of the hoop stress.

However, widely used design codes for composite repair, such as ASME PCC-2 [4] and ISO 24817 [5], often result in conservative designs. These codes assume full-

circumferential and infinitely long corrosion defects, underestimating the required thickness of the composite repair in certain cases. Finite element analysis (FEA) has proven to be an effective tool for predicting the burst capacity of composite-repaired corroded pipelines. Various studies have utilized FEA to investigate factors such as temperature effects, bonding conditions, and repair dimensions [6, 7, 8, 9].

Full-scale tests have also been conducted to examine the burst capacity of CRC pipelines, considering different pipe dimensions and defect geometries [6, 7]. These tests have shown variations in burst capacity based on the defect type, width, and material properties. Existing models for predicting the burst capacity of corroded pipelines, such as the ASME B31G and B31G Modified models, consider defect depth and length but ignore defect width.

Since the composite material has reinforcement in a specific direction, it is considered an orthotropic elastic material with the plane stress condition. This is defined in Abaqus as *Lamina*. The corresponding stress-strain relationship is given by Eq. (1.1) [7], where ε_{ij} and σ_{ij} denote the strains and stresses in the local coordinate system of the composite (i, j = 1, 2); E_1 and E_2 are Young's moduli in 1 and 2 directions, respectively; ν_{12} is Poisson's ratio, and G_{12} = is the shear moduli of the composite material.

$$\begin{Bmatrix} \varepsilon_{11} \\ \varepsilon_{22} \\ \varepsilon_{12} \end{Bmatrix} = \begin{bmatrix} 1/E_1 & -\nu_{12}/E_1 & 0 \\ -\nu_{12}/E_1 & 1/E_2 & 0 \\ 0 & 0 & 1/(G_{12}) \end{bmatrix} \begin{Bmatrix} \sigma_{11} \\ \sigma_{22} \\ \sigma_{12} \end{Bmatrix} \tag{1.1}$$

For composite materials, the Tsai-Wu [4] and Hashin [10] damage criteria are the most commonly used. The Hashin criterion is considered in this study because it is more advantageous than the Tsai-Wu criterion since the former is based on a system of equations and considers the failure in both the matrix and the fibre, whereas the latter is based on a single failure mode. Four damage indices are included in the Hashin criterion, i.e. FTCRT, FCCRT, MTCRT and MCCRT, corresponding to the fibre tension, fibre compression, matrix tension and matrix compression failures, respectively. For CRC pipelines, only FTCRT and MTCRT, i.e. fibre and matrix tension failures, are relevant.

The design equations consider one failure mode that is in the composite repair and in the circumferential direction. Investigations [11] have shown that, depending on the properties of the materials and the shape of the defect, three failure modes can occur on composite-repaired corroded pipelines. These complexities are currently not being considered on the existing models and leads to inaccuracies in certain cases.

1.2 Objective

The main objectives of this thesis are summarized as follows:

1) Validate the FEA model assumptions, material characterization and failure modes using the results of the full-scale tests in literature.

2) Investigate the effect that the defect width has on the burst capacity, and the correlation between this parameter and the other defect dimensions (defect length and depth)

3) Quantify the defect width effect and the relation with a CRC pipeline with a full-circumferential defect

4) Propose a correction factor to account for the defect width effect on this case

5) Perform an extensive parametric analysis using the FEA validated model

6) Developed a machine learning model to predict the burst capacity of CRC pipelines, using Gaussian process regression (GPR) and the FEA cases of the parametric analysis

7) Evaluate the parameters that affect the burst capacity that are currently not considered on the prediction model

1.3 Scope

Given the limitations and inaccuracies in current prediction models, this thesis aims to provide insights into the parameters affecting burst capacity and propose improvements to predict the burst capacity of composite-repaired corroded pipelines. The main topics are

presented in chapters 2 and 3. Chapter 2 presents the validation of the FEA model using 11 cases of the existing literature, the parametric analysis of 60 cases with different defect geometries, and the investigation of the defect width effect on the burst capacities. Based on the results, a correction factor is proposed for this scenario. Chapter 3 presents a wider parametric analysis (864 FEA cases) where different material properties are considered. Then, these cases are divided into a regression set to train the GPR model and a test set for validation. Finally, the importance of each input parameter in the calculation of the burst capacity is evaluated as well.

1.4 Thesis format

This thesis is prepared in an Integrated-Article Format as specified by the School of Graduate and Postdoctoral Studies at Western University. Chapter 1 presents a background on composite pipeline repair and the existing models limitations. Chapters 2 and 3 are the main chapters of the thesis and focus on the investigation of the prediction of the burst capacity of CRC pipelines using two different methods. Finally, chapter 4 presents the conclusions and recommendations for future studies.

References

[1] F.G. Alabtah, E. Mahdi, F.F. Eliyan. The use of fibre reinforced polymeric composites in pipelines: a review. Composite Structures 276 (2021) 114595

[2] American Society of Mechanical Engineers. Non Metallic and Bonded Repairs. In ASME PCC-2-2018 Repair of Pressure Equipment and Piping: An American national standard (2018)

[3] International Standard Organization. ISO-24817 Petroleum, petrochemical and natural gas industries: composite repairs for pipework: Qualification and design, installation, testing and inspection (2017)

[4] L. Meniconi, J. Freire, R. Vieira, J. Diniz. Stress analisis of pipelines with composite repairs. Proceedings of the 2002 4th International Pipeline Conference (2002) 2031-2037

[5] F. Al Abtah, E. Mahdi, S. Gowid. The use of composite to eliminate the effect of welding on the bending behaviour of metallic pipes. Composite structures 235 (2020) 111793

[6] H. da Costa Mattos, J.M. Reis, M. Da Silva, F. Amorim, V. Perrut. Analysis of a glass fibre reinforced polyurethane composite repair system for corroded pipelines at elevated temperatures. Composite structures 114 (2014) 117-123

[7] P.H. Chan, K.Y. Tshai, M. Johnson, L.H. Choo, S. Li, K. Zakaria. Burst strength of carbon fibre reinforced polyethylene strip pipeline repair system – a numerical and experimental approach. Journal of Composite Materials 49(6) (2015) 749-756

[8] A. Ali, M. Zahiraniza, M. Thar. Burst capacity of pipe under corrosion defects and repaired with thermosetting liner. Steel and composite structures 35(2) (2020) 171-186

[9] J. Chen, H. Wang, M. Salemi, P.N. Balaguru. Finite element analysis of composite repair for damaged steel pipeline. Coatings 11(3) (2021) 301

[10] Z. Hashin. Failure criterion for unidirectional fiber composites. Journal of applied mechanics 47(2) (1980) 329-334

[11] D. Kong, X. Huang, M. Xin, G. Xian. Effects of defect dimensions and putty properties on the burst performances of steel pipes wrapped with CFRP composites. The International Journal of Pressure Vessels and Piping 186 (2020) 104-139

Chapter 2

2 Investigation of the Defect Depth on the Burst Composite-Repaired Pipelines with Corrosion Defects Using Finite Element Analysis

2.1 Introduction

There are thousands of kilometres of buried steel oil and gas pipelines that form a key part of the critical infrastructure systems for modern societies. Many pipelines in Canada and around the world have had long service lives and are degrading over time. A main degradation mechanism for steel pipelines is corrosion, which leads to localized loss of the pipe wall thickness and hence compromises the capacity of the pipeline to contain the high operating pressure.

Composite repair is a method to rehabilitate pipelines that have suffered damages or degradations. It involves the application of a composite material to the affected pipe segment. The composite material is applied to the exterior of the substrate and is designed to bond with the pipe surface, creating a strong, protective layer that can reinforce the pipe and restore its structural integrity. The composite material is usually applied using a hand lay-up process of pre-impregnated sheets of glass or carbon fibre and cured on site. Composite repair is a cost-effective and efficient method for repairing damaged pipes, as it can be applied quickly and with minimal disruption to operations. It is also a durable and long-lasting solution, as the composite material is resistant to corrosion, abrasion and other forms of wear and tear [1].

According to studies reported in [2, 3], widely used design codes for the composite repair such as ASME PCC-2 [4] and ISO 24817 [5] result in conservative designs. The approaches recommended in the ASME code assume that no defect dimension is known other than the remaining wall thickness of the substrate. Therefore, it is assumed in the code that the corrosion defect is full-circumferential and infinitely long such that the remaining strength of the corroded pipeline is computed as a thin-walled pipe with a thickness equal to that of the remaining ligament. The required strength of the composite repair to restore the pipe capacity can then be determined. However, test results reported

by Da Mattos et al. [6] demonstrated that both ASME and ISO codes can lead to the required thickness of composite being underestimated in certain cases.

The finite element analysis (FEA) has been shown in the literature to be an effective tool to predict the burst capacity of composite-repaired corroded (CRC) pipelines. Da Mattos et al. [6] used FEA to investigate the temperature effect on the ultimate hoop resistance of fibre-reinforced polymer (FRP). Chan et al. [7] carried out FEA of subsea pipelines repaired using carbon fibres. Ali et al. [8] performed full-scale tests and FEA analyses of CRC pipe specimens and found a good agreement between the test and FEA results. Chen et al. [9] carried out FEA to study the effect of limiting the repair dimension in the hoop direction (i.e. using a patch repair instead of a wrap repair) and the bonding conditions.

Full-scale tests have been conducted to investigate the burst capacity of CRC pipelines under internal pressure for different pipe dimensions and defect geometry [2,3,6,7,8,10]. Duell et al. [3] conducted two full-scale burst tests of CRC pipe specimens with an outside diameter of 168 mm, one with a full-circumferential defect and the other with a localized defect. All the other dimensions of both the pipe specimen and composite repair were kept the same on the two tests. The results showed that the burst capacity of the specimen with the full circumferential defect is 2% greater than that of the specimen with the localized defect. On the other hand, Kong et al. [10] reported that the burst capacity of a specimen with a full-circumferential defect was 23.6% lower than that of the specimen with a 10 mm wide defect (all else being the same). The main difference between the two experiments mentioned earlier is the use of a high hoop resistant and high elastic modulus composite material in [10], which results in very thin composites that failed due to the transverse tension in the matrix rather than the hoop stress in the fibre.

A corrosion defect on the pipeline is quantified by three dimensions: length in the pipe longitudinal direction, width in the pipe circumferential direction and depth in the through wall thickness direction. Well known models to predict the burst capacity of corroded pipelines such as the ASME B31G and B31G Modified models [11] take into account the defect depth and length but ignore the defect width. Zhang and Zhou [12] investigated the

effect of the defect width on the burst capacity of corroded pipelines and reported that a greater defect width leads to a higher burst capacity (all else being the same).

Previous studies provide insufficient understanding of the defect width effect on the burst capacity of CRC pipelines. The objective of this study is to carry out parametric FEA to evaluate the impact of the defect width on the burst capacity of CRC pipelines and incorporate the defect width effect into the burst capacity model for CRC pipelines to improve its accuracy. The study is focused on CRC pipelines that are subjected to internal pressure only and contain corrosion defects on the pipe external surface with depths up to 80% of the pipe wall thickness.

The rest of the paper is organized as follows. Section 2.2 presents details of the FEA and full-scale burst tests collected from the literature for the validation of the finite element model. Section 2.3 presents results of the parametric FEA and the defect width effect on the burst capacity of CRC pipelines. Section 2.4 describes the burst capacity model recast from the design equation specified in ASME PCC-2 [4] and evaluates the predictive accuracy of the model based on results of the parametric FEA. A defect width correction factor is proposed to be incorporated in the burst capacity model. The proposed correction factor is also discussed in the context of its practical application in the design and analysis of FRP repair of corroded pipelines. Finally, concluding remarks are given in Section 2.5.

2.2 FEA model

2.2.1 General

Composite repairs consist of three basic components: the substrate, putty and FRP. The substrate is the surface to which the composite repair will be applied (i.e. the corroded steel pipeline section); the putty is a filler material used to create a smooth surface on top of the substrate, and FRP is the composite material used to repair the damaged pipe.

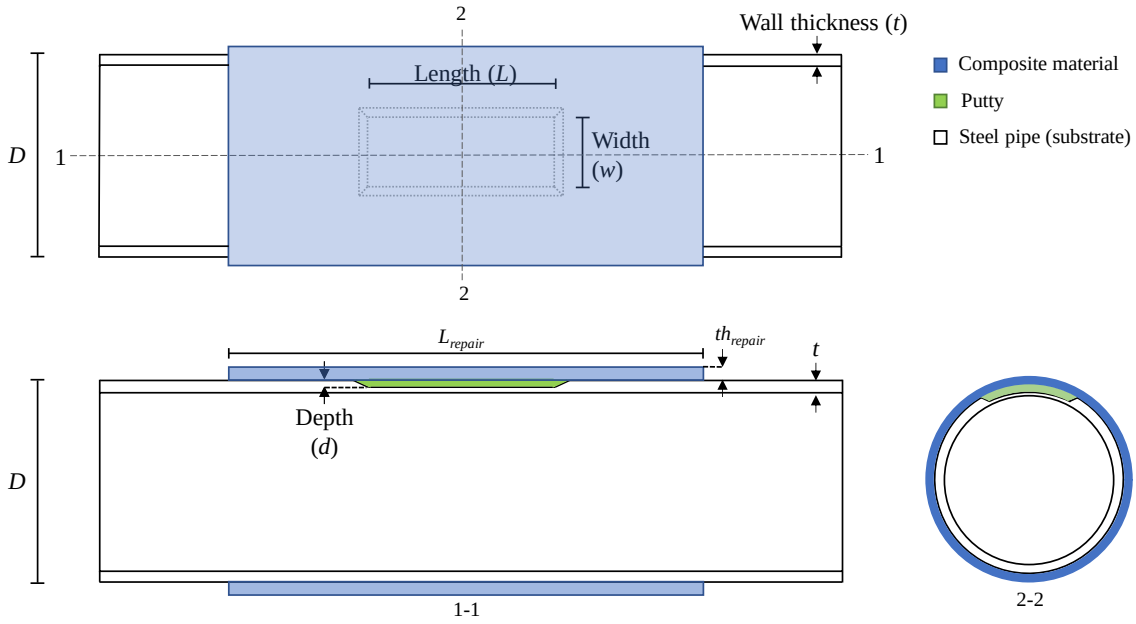

Figure 2.1: Schematics of CRC pipelines with a localized defects

Figure 2.1 illustrates the basic components of a CRC pipe section. In this figure, D is the pipe outside diameter; t is the pipe wall thickness; L, w and d denote the defect length, width and depth, respectively, and L_{repair} and th_{repair} are the length and thickness of the composite repair, respectively.

The basic design approach of CRC pipelines is that the hoop stress in the defect area is mechanically transferred from the substrate to the composite sleeve. Results from [13, 14] indicate that up to the substrate yielding, the substrate carries most of the hoop stress due to the steel's high elastic modulus. After yielding, the composite reinforcement starts to carry a more substantial part of the hoop stress. Fig. 2.2 depicts the change in the von Mises stress in the steel in the defect and defect-free areas of a CRC pipe specimen as the internal pressure increases. It can be observed that at first (during the elastic response) the steel in the defect area is under a higher stress than the steel outside the repair area. Once yielding of the steel starts, the composite wrapping the corroded region of the steel adds an external pressure to the substrate, which reduces the stress in the steel in this region.

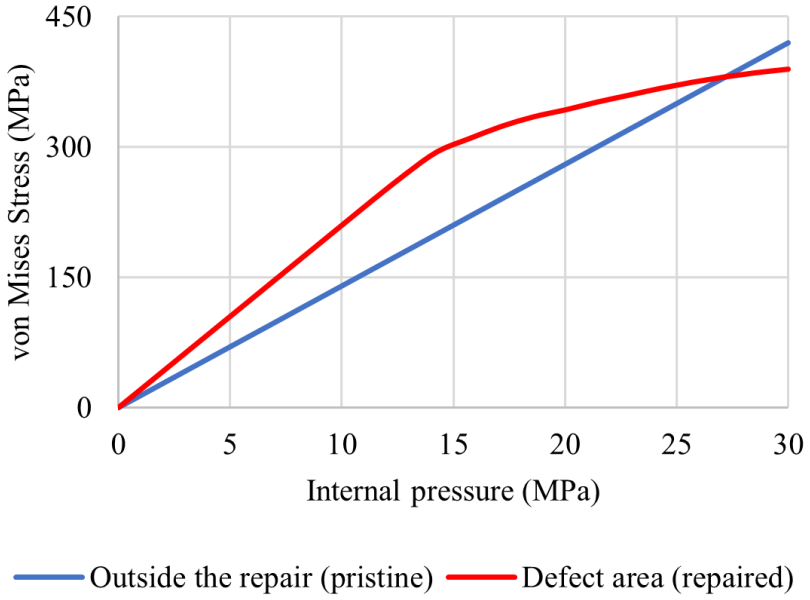

Figure 2.2 von Mises stress on steel in the defect and outside the repair areas of a CRC pipe specimen

The commercial finite element package Abaqus 2020 is used to carry out FEA in the present study. Full-scale tests are collected from the literature and used to validate the finite element models including the stress-strain relationships for both steel and FRP, the interface boundary conditions between steel and FRP, and the failure criterion adopted to determine the burst capacity of the pipeline. To reduce the number of elements and improve the computational efficiency, symmetry along the XY plane (i.e. axial direction) is considered.

2.2.2 Model Specifics

The steel is modelled as an isotropic material using the C3D8R solid element (i.e. the 8-node linear brick element with reduced integration points). The true stress (σ) – true strain (ε) relationship of the steel is assumed as follows [12]:

$$\sigma = E\,\varepsilon \quad \sigma < \sigma_y \tag{2.1}$$

$$\sigma = K\varepsilon^n \quad \sigma \geq \sigma_y \tag{2.2}$$

where E is Young's modulus; σ_y denotes the yield strength, and K and n are the coefficients of the power-law stress-strain relationship in the plastic domain and can be determined from the coupon tensile test data. If such test data is unavailable, n can be estimated using the following empirical equation proposed in [15].

$$n = 0.239\left(\frac{1}{\sigma_y/\sigma'_{uts}} - 1\right)^{0.596} \tag{2.3}$$

where σ'_{uts} is the ultimate tensile strength (engineering stress). Eq. (2.4), which is derived based on Considere´s criterion [16], can be used to calculate K as,

$$K = \frac{e^n}{n^n}\sigma'_{uts} \tag{2.4}$$

Fig. 2.3 depicts the finite element model of a CRC pipeline with a representative mesh configuration, which has a high mesh density in the defect area and transitions to a low mesh density in the defect-free area. The boundary conditions of the model consist of translational restrictions in the axial direction at one end of the specimen and symmetry boundary conditions on the XY plane.

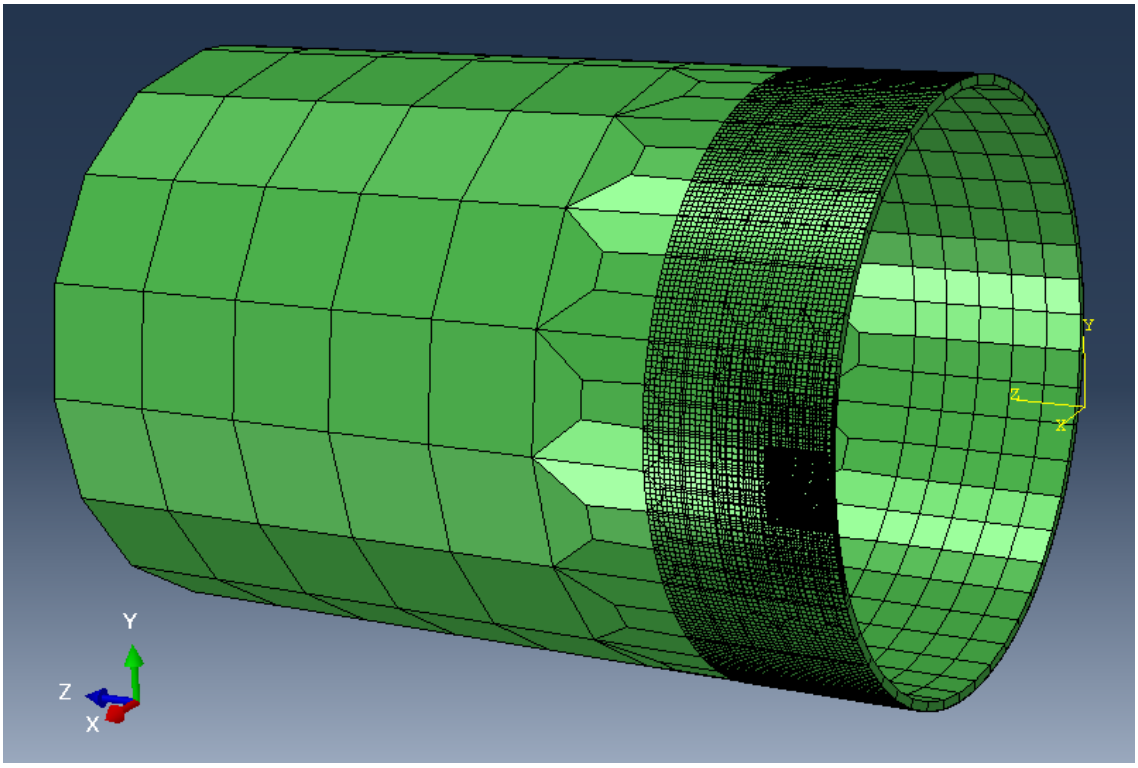

Figure 2.3 Abaqus model of a CRC Pipeline

Many polymeric materials with high compression strengths are suitable choices for putty. In this study, putty is characterized as an isotropic elastic material and modelled using the C3D8R element. The properties required for modelling the putty are its elastic modulus (E_p) and Poisson's ratio (ν_p). A parametric study reported in [9] indicates that the elastic modulus of the putty has a minor effect on the burst capacity of the CRC pipeline.

The composite material or FRP includes a polymer matrix that binds the fibre (reinforcement). Mechanical properties of the composite material can be obtained by performing mechanical tests on specimens made with the same materials, thickness, composition and angle of orientation of the reinforcement. In this study, the composite sleeve is modelled using the S4R (4-node curved shell element with reduced integration) elements in Abaqus. It is assigned with a composite layup to define the thickness and properties of each ply. Fig. 2.4(a) depicts a composite layup for a case with six layers of 0.52 mm thickness each. Each layer or ply has specific thickness, material, and orientation. Fig. 2.4(b) illustrates the axes of the global (i.e. X, Y and Z) and local coordinates (i.e. 1,

2 and 3) for the composite layup as a shell element in Abaqus. Note that the local axis 1 is in the hoop direction of the pipe (longitudinal direction of the FRP repair), and the local axis 2 is in the axial direction of the pipe (transverse direction of the FRP repair).

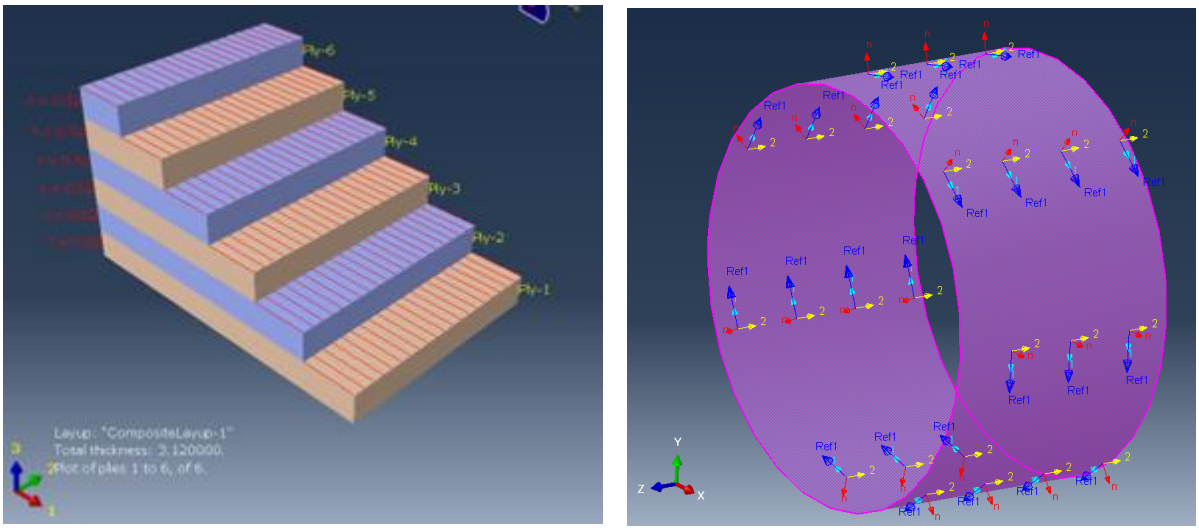

(a) Composite layup section (b) Composite layup element

Figure 2.4 FRP repair model as a composite layup un Abaqus v2020

Since the composite material has reinforcement in a specific direction, it is considered an orthotropic elastic material with the plane stress condition. This is defined in Abaqus as *Lamina*. The corresponding stress-strain relationship is given by Eq. (2.5) [7], where ε_{ij} and σ_{ij} denote the strains and stresses in the local coordinate system of the composite (i, j = 1, 2); E_1 and E_2 are Young's moduli in 1 and 2 directions, respectively; ν_{12} is Poisson's ratio, and G_{12} = is the shear moduli of the composite material.

$$\begin{Bmatrix} \varepsilon_{11} \\ \varepsilon_{22} \\ \varepsilon_{12} \end{Bmatrix} = \begin{bmatrix} 1/E_1 & -\nu_{12}/E_1 & 0 \\ -\nu_{12}/E_1 & 1/E_2 & 0 \\ 0 & 0 & 1/(G_{12}) \end{bmatrix} \begin{Bmatrix} \sigma_{11} \\ \sigma_{22} \\ \sigma_{12} \end{Bmatrix} \tag{2.5}$$

The material stability for the plane stress condition requires that:

$$|\nu_{12}| < (E_1/E_2)^{1/2} \tag{2.6}$$

Different criteria have been proposed in the literature to define failure of CRC pipelines in FEA. In general, the failure criterion considers failures of the steel substrate and FRP

repair. For the substrate, [16] has demonstrated the effectiveness of the criterion whereby failure is defined as the point at which the maximum nodal von Mises (true) stress within the corrosion defect region reaches the true stress corresponding to the ultimate tensile strength of the pipe steel. This criterion is adopted in the present study. For FRP, the Tsai-Wu [13] and Hashin [19] damage criteria are the most commonly used.

The Hashin criterion is considered in this study because it is more advantageous than the Tsai-Wu criterion since the former is based on a system of equations and considers the failure in both the matrix and the fibre, whereas the latter is based on a single failure mode. Furthermore, the Hashin criterion is a built-in option in Abaqus. Four damage indices are included in the Hashin criterion, i.e. FTCRT, FCCRT, MTCRT and MCCRT, corresponding to the fibre tension, fibre compression, matrix tension and matrix compression failures, respectively. For CRC pipelines, only FTCRT and MTCRT, i.e. fibre and matrix tension failures, are relevant. These two indices are calculated as follows:

$$\text{FTCRT} = \left(\frac{\hat{\sigma}_{11}}{X_T}\right)^2 + \alpha\left(\frac{\hat{\sigma}_{12}}{S_L}\right)^2 \tag{2.7}$$

$$\text{MTCRT} = \left(\frac{\hat{\sigma}_{22}}{Y_T}\right)^2 + \left(\frac{\sigma_{12}}{S_L}\right)^2 \tag{2.8}$$

where $\hat{\sigma}_{11}$ (≥ 0), $\hat{\sigma}_{22}$ (≥ 0) and $\hat{\sigma}_{12}$ are components of the effective stress tensor; α is a coefficient that determines the contribution of the shear stress; X_T, Y_T and S_L are the longitudinal tensile strength, transverse tensile strength, and longitudinal shear strength of FRP, respectively. If either FTCRT or MTCRT reaches unity, failure of the composite is reached. The values of $\hat{\sigma}_{11}$, $\hat{\sigma}_{22}$, and $\hat{\sigma}_{12}$ are calculated by multiplying the corresponding stress tensor components (i.e. σ_{11}, σ_{22} and σ_{12}) with a damage factor [17]. Prior to any damage it can be assumed that $\hat{\sigma}_{ij} = \sigma_{ij}$ (i, j = 1, 2) [17], which is consistent with the analysis carried out in the present study as the analysis ends once damage is initiated. Hashin [17] pointed out that Eq. (2.7) can be simplified with an adequate accuracy by assuming α = 0, which results in FTCRT being defined by,

$$\text{FTCRT} = \left(\frac{\hat{\sigma}_{11}}{X_T}\right)^2 \tag{2.9}$$

It follows that failure occurs if $\hat{\sigma}_{11}$ equals X_T.

2.2.3 Model validation

The finite element model described in the previous section is validated based on tests of CRC pipe specimens. To this end, a total of eleven specimens are collected from the literature. Table 2.1 summarizes the pipe attributes and sizes of the corrosion defects in the specimens. The properties of the steels and putty materials of the specimens are presented in Table 2.2, and properties of the FRP are summarized in Table 2.3.

Table 2.1 Summary of 11 full-scale tests for validation of the finite element model

No.	Specimen ID	*D* (mm)	*t* (mm)	*d/t*	*L* (mm)	*w* (mm)	th_{repair} (mm)	Source
1	1	219	12.7	0.5	622	c*	1.8	[7]
2	1	273	9.3	0.6	152	100	26	[18]
3	2	324	9.5	0.75	200	150	26	[18]
4	4	219	6.0	0.6	133	102	6.2	[19]
5	1	168	7.1	0.5	100	100	3.1	[2]
6	3	102	2.1	0.5	30	40	5	[20]
7	C10-LAStress-Tc	168	7.1	0.72	200	10	2.6	[10]
8	C10-LAStrain-Tc	168	7.1	0.72	200	10	1	[10]
9	CC-LAStress-Tc	168	7.1	0.72	200	c	2.6	[10]
10	Axisymmetric	168	7.1	0.5	152	152	3.1	[3]
11	6x6	168	7.1	0.5	152	c	3.1	[3]

*: The corrosion defect is full-circumferential (i.e. covers the entire circumference of the pipe)

Table 2.2 Properties of steels and putty of the 11 full-scale test specimens

No.	Steel				Putty	
	σ_y (MPa)	σ'_{uts} (MPa)	K (MPa)	n	E_p (GPa)	v_p
1	358	500	711	0.110	8.95	0.24
2	289	369	526	0.111	3.00	0.28
3	289	369	526	0.111	3.00	0.28
4	305	520	700	0.158	3.30	0.37
5	293	503	786	0.183	18.93	0.28
6	242	482	860	0.238	1.43	0.15
7	300	450	693	0.155	1.80	0.28
8	300	450	693	0.155	1.80	0.28
9	300	450	693	0.155	1.80	0.28
10	300	560	995	0.220	1.74	0.45
11	300	560	995	0.220	1.74	0.45

Table 2.3 Properties of materials used for composite repair on the full-scale tests used for validation

No.	Fibre type	E_1 (GPa)	E_2 (GPa)	v_{12}	G_{12} (MPa)	X_T (MPa)	Y_T (MPa)	S_L (MPa)
1	Carbon fibre	141	14.1	0.34	75.46	1128	27	80
2	Glass fibre	30	6	0.28	3.2	300	35	72
3	Glass fibre	30	6	0.28	3.2	300	35	72
4	Glass fibre	48.47	6.8	0.1	3.2	678	34.4	45.8
5	Glass fibre	14.32	10.1	0.28	3.2	241	35	72
6	Glass fibre	17	5	0.189	2.72	510	35	72
7	Carbon fibre	250	7.2	0.362	4500	2800	28	49
8	Carbon fibre	250	7.2	0.362	4500	2800	28	49
9	Carbon fibre	250	7.2	0.362	4500	2800	28	49
10	Carbon fibre	49	23.4	0.43	690	576	27	80
11	Carbon fibre	49	23.4	0.43	690	576	27	80

For the validated model, a comprehensive mesh analysis was conducted to ensure optimal mesh sizing across various sections of the model. Mesh adequacy was established by considering cases where transitioning to a finer mesh yielded a change of less than 0.5%. The initial step involved determining the steel's maximum mesh size, both within the repair zone and on the defect area, where a finer mesh was deemed necessary. Utilizing these two values, a seamless transition was formulated. Subsequently, an evaluation of the putty's mesh size was performed, accounting for its impact on the FRP component. The objective was to accurately simulate load transfer to the FRP, necessitating a well-fitted putty mesh. Lastly, the mesh size of the composite repair was evaluated.

The FEA-predicted and actual burst capacities (P_{FEA} and P_{test}) for the 11 specimens are summarized in Table 4, together with the observed failure modes of the specimens obtained from the respective sources. As show in Table 2.4, the mean and coefficient of variation (COV) of P_{test}/P_{FEA} for the 11 specimens are 1.01 and 3.5%, respectively. Furthermore, the predicted failure modes agree with the observed failure modes for all 11 specimens. These results provide a strong validation of the finite element model and failure criteria employed in the present study. As an example, Figs. 2.5(a), 2.5(b) and 2.5(c) depict, respectively, the fibre tension (FTCRT), matrix tension (MTCRT) and steel failure modes for specimens #7, #8 and #9 predicted by FEA, which agree with the actual failure modes as depicted in Fig. 7 of Ref. [10].

Table 2.4 Validation of FEA model using available full-scale tests

No.	P_{test} (MPa)	P_{FEA} (MPa)	P_{test}/P_{FEA}	Observed failure mode
1	53.5	53.9	0.99	FTCRT (fibre tension)
2	30.0	30.3	1.04	Steel (outside repair)
3	24.4	24.1	1.04	FTCRT
4	29.1	27.7	1.05	FTCRT
5	33.0	34.1	0.97	FTCRT
6	18.0	18.8	0.96	FTCRT
7	42.5	44.0	0.97	FTCRT
8	47.8	47.0	1.02	Steel

9	36.5	34.4	1.06	MTCRT (matrix tension)
10	43.8	42.7	1.03	FTCRT
11	43.1	43.1	1.00	FTCRT
Mean			1.01	
COV			3.5%	

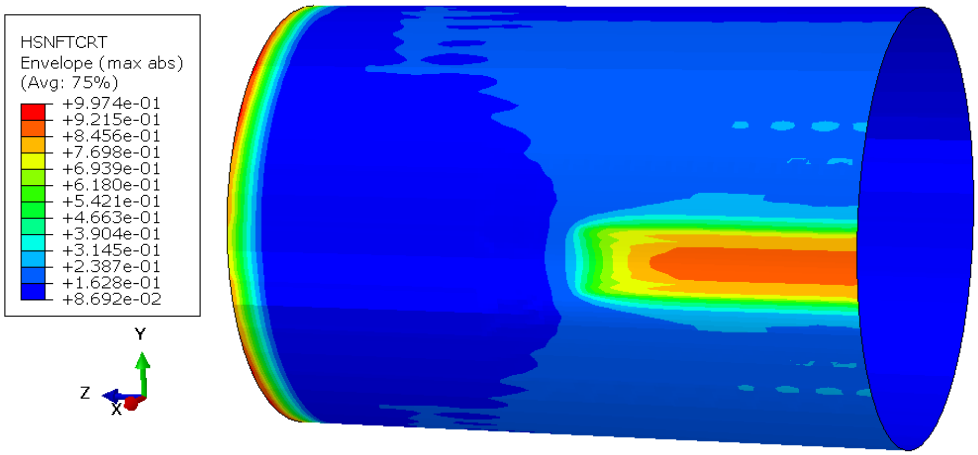

(a) Fibre tension failure mode (FTCRT)

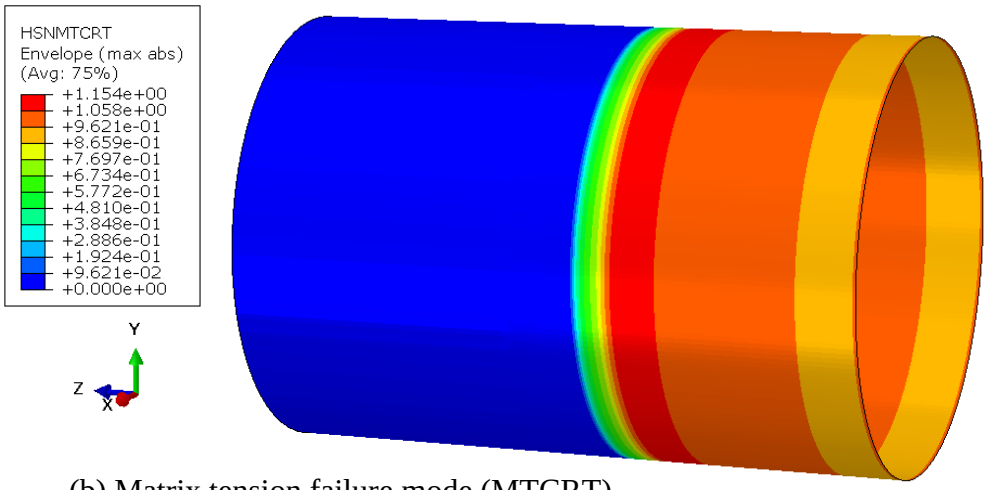

(b) Matrix tension failure mode (MTCRT)

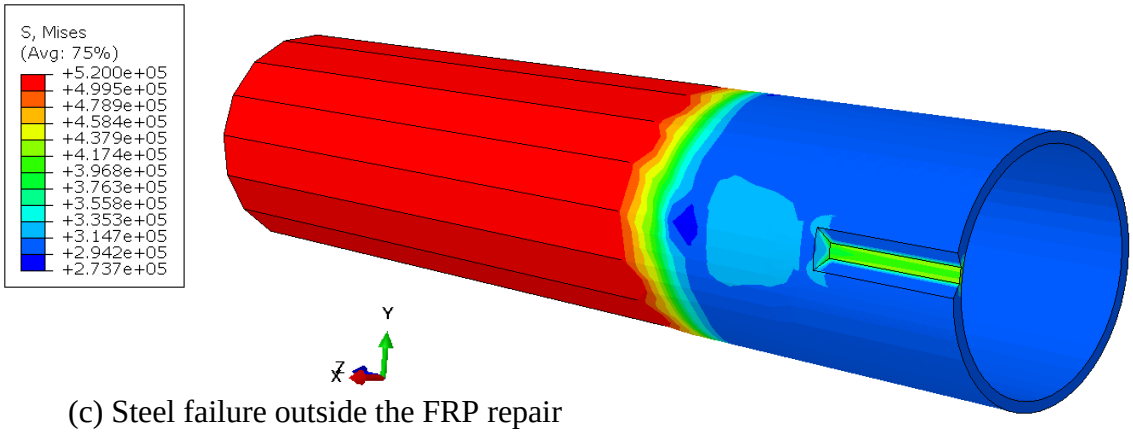

(c) Steel failure outside the FRP repair

Figure 2.5 Three failure modes found on full-scale tests of CRC pipelines

2.3 Effect of defect width on burst capacity of CRC pipelines

2.3.1 Parametric FEA cases

The pipe considered in the parametric analysis has D = 457 mm and t = 7.11 mm, and the yield and tensile strengths (σ'_{uts}) of the pipe steel are assumed to be 455 and 631 MPa, respectively. The value of E is assumed to be 2.1×10^5 MPa, and coefficients of the stress-strain relationship in the plastic domain, K and n, are estimated to be 799 MPa and 0.104 using Eqs. (2.3) and (2.4), respectively. The normalized defect depth ($d' = d/t$) is assumed to be 0.3, 0.5 or 0.7; the normalized defect length ($L' = L^2/(Dt)$) is assumed to be 0.5, 2, 5 or 20, and the normalized defect width ($w' = w^2/(Dt)$) is also assumed to be 0.5, 2, 5 or 20. This results in a total of 48 localized defects with different combinations of the depth, length and width. For each combination of the defect depth and length, a full circumferential defect is included for comparison. This results in a total of 12 cases with full circumferential defects.

The material used for the composite repair is assumed to be an epoxy polymer with fibreglass reinforcement. The elastic moduli in the hoop (E_1) and axial (E_2) directions of the composite material are assumed to be 10.5 GPa and 1.05 GPa respectively. The shear modulus G_{12} is 3.2 GPa as commonly reported in literature for fibreglass. The longitudinal tensile strength (i.e. in the hoop direction) (X_T) is assumed to be 105 MPa, which corresponds to a failure strain of 1.0% [3, 10, 13]. The transverse tensile strength and longitudinal shear strength (S_L and Y_T) are assumed to be 35 and 72 MPa respectively [21]. The putty is assumed to have an elastic modulus (E_p) of 2400 MPa and Poisson's ratio (ν_p) of 0.28. The Hashin failure criterion for FRP is adopted.

2.3.2 Results

The predicted burst capacity of a pipe with a full circumferential defect (P_{circ}) is used as the basis to quantify the width effect on the burst capacity of pipes with localized defects (P_w). Fig. 2.6 depicts P_w/P_{circ} as a function of the normalized width of the localized defect. Fig. 2.6 indicates that the burst capacity of a CRC pipe with a localized defect is lower than that of the CRC pipe with a full circumferential defect of the same depth and length. The

values of P_w/P_{circ} range between 0.52 and 0.92 depending on the depth, length and width of the localized defect. It can be observed from Fig. 2.6 that the reduction in the burst capacity due to the width effect is greater for deeper defects.

(d) $L´ = 20$

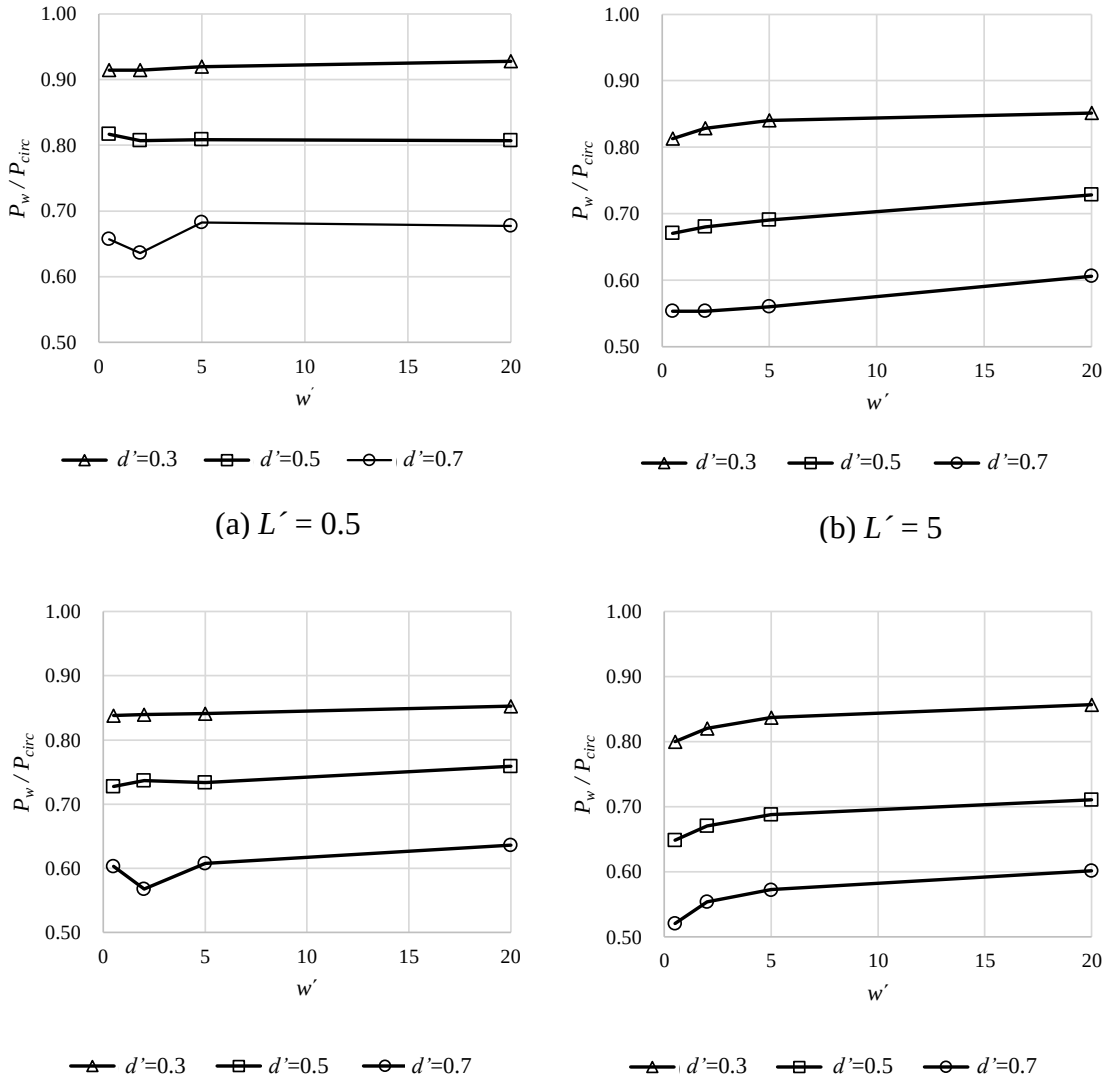

(a) $L´ = 0.5$ (b) $L´ = 5$

(c) $L´ = 2$ (d) $L´ = 20$

Figure 2.6 Width effect on the burst capacity of CRC pipelines

If the defect is short (e.g. $L^{'} = 0.5$), P_w/P_{circ} corresponding to the same d' is practically the same for different values of w'. For long and deep defects (e.g. $L^{'} = 20$ and $d' = 0.7$), P_w/P_{circ} decreases from 0.6 to 0.52, i.e. a decrease of 13% in the burst capacity, as w' decreases from 20 to 0.5. This decrease in the burst capacity is explained using Fig. 2.7.

Fig. 2.7 compares the von Mises (VM) stresses in the substrate and hoop strains in the composite repair of two CRC pipes, one with a localized defect with $w' = 5$ and one with a full circumferential defect. For both pipes, $d' = 0.5$, $L' = 5$, and the internal pressure is 13.5 MPa.

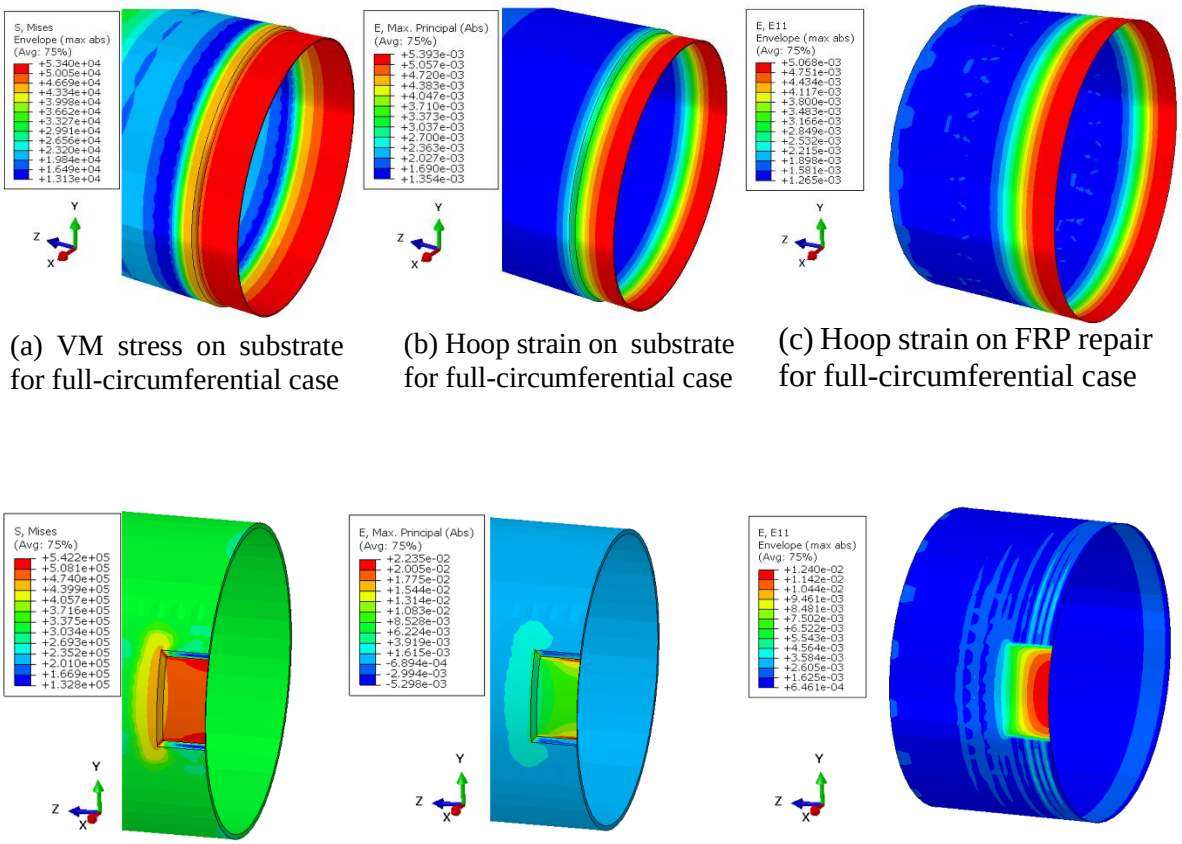

(a) VM stress on substrate for full-circumferential case

(b) Hoop strain on substrate for full-circumferential case

(c) Hoop strain on FRP repair for full-circumferential case

(d) VM stress on substrate for localized defect case

(e) Hoop strain on substrate for localized defect case

(f) Hoop strain on FRP repair for localized defect case

Figure 2.7 Stress and strain distribution on a CRC pipeline with a circumferential and a localized defect

Figs. 2.7(a) and 2.7(b) show that the stress and strain in the substrate of a CRC pipeline with a full circumferential defect distributes uniformly without concentrations. On the other hand, Figs. 2.7(d) and 2.7(e) show that on a CRC pipeline with a localized defect, the stress and strain in the substrate are concentrated at the edges of the defect, which is due to bulging and causes high stress and strain in the FRP.

Figs. 2.7(b) and 2.7(e) show that at the same internal pressure, the maximum strain in the substrate of the specimen with the localized defect is markedly higher than that of the specimen with the full circumferential defect as the former specimen undergoes more significant bulging than the latter. As a result of the bulging, the hoop strain and stress of the composite repair, which govern its failure, are markedly higher in the pipe with the localized defect than those in the pipe with the full circumferential defect. Figs. 2.7(c) and 2.7(f) show that at the same internal pressure, the hoop strain in the composite of the CRC pipe with a localized defect is more than twice that of the CRC pipe with the full circumferential defect. Fig. 2.8 depicts the maximum hoop stresses in the composite repair for four CRC pipes containing localized defects with *w'* equal to 0.5, 2, 5 and 20, respectively, at the internal pressure of 13.5 MPa, and a CRC pipe containing a full circumferential defect at the same internal pressure. This figure clearly shows that the maximum hoop stress in the composite decreases, i.e. due to less severe bulging, as *w'* increases for the pipes with localized defects. The maximum hoop stress in the composite of the pipe with the full circumferential defect is the lowest of the five pipes considered. The results suggest that the composite repair is more effective for pipes with full circumferential defects than for those with localized defects.

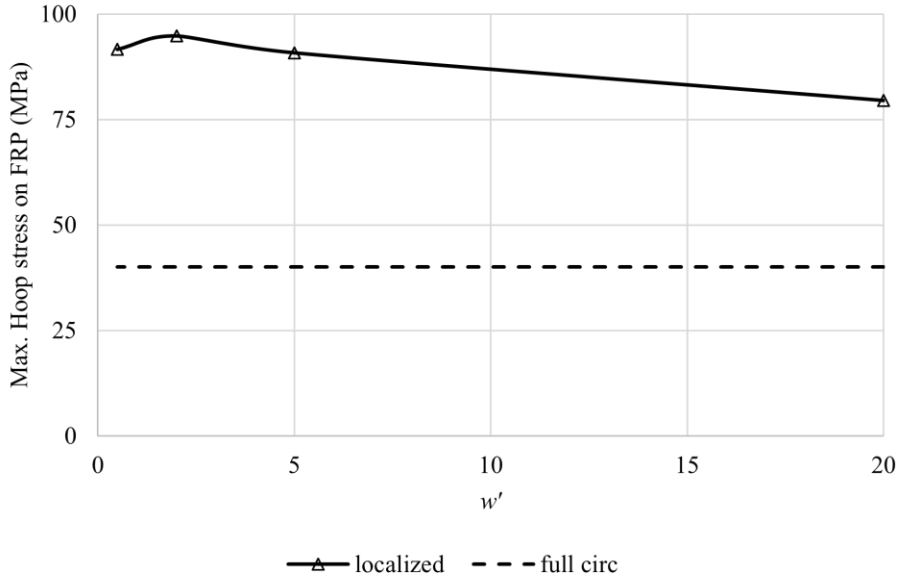

Figure 2.8 Comparison between the hoop stresses in FRP at the same pressure in localized and full-circumferential defects under the same conditions

2.4 Incorporation of the width effect on burst capacity model

2.4.1 Burst capacity of ASME PCC-2 designed CRC pipelines

Part 4 of the ASME PCC-2 code [4] includes two approaches to calculate the minimum thickness of FRP repair for CRC pipelines. The first approach assumes that the only defect dimension known is the defect depth. It further assumes that the substrate is elastic-perfectly plastic and yields when the burst capacity of the CRC pipe is reached. The second approach is based on the well-known ASME B31G model for calculating the burst capacity of a corroded pipeline by taking into account the defect depth and length in the calculation. The first approach is considered in the present study. By recasting the design equation to predict the burst capacity, the burst capacity based on the ASME PCC-2 code, $P_{PCC\text{-}2}$, is written as

$$P_{PCC-2} = \frac{2}{D}\left(th_{repair}X_T + \sigma_y t_s\right) \tag{2.10}$$

where $t_s = t - d$ is the remaining thickness of the substrate on the defect area. Eq. (2.10) is derived based on the well-known Barlow equation by considering the contributions of the composite (i.e. the $th_{repair}X_T$ term in Eq. (2.10)) and the substrate (i.e. the $\sigma_y t_s$ term in Eq. (2.10)) to the burst capacity.

2.4.2 Accuracy of ASME PCC-2 model based on FEA results

The parametric FEA results presented in the previous section are used to evaluate the accuracy of the burst capacity model, i.e. Eq. (2.10), derived based on the ASME PCC-2 recommendation. Figure 2.9 depicts $P_{FEA}/P_{PCC\text{-}2}$ for the 60 FEA cases of localized and full circumferential defects described in Section 2.3.1. The figure clearly shows that Eq. (2.10) is accurate for full-circumferential defects but can be markedly non-conservative for localized defects. The mean and COV of $P_{FEA}/P_{PCC\text{-}2}$ for the cases with localized defects and full-circumferential defects, respectively, are summarized in Table 2.5, which clearly indicates the inadequacy of $P_{PCC\text{-}2}$ for cases with localized defects.

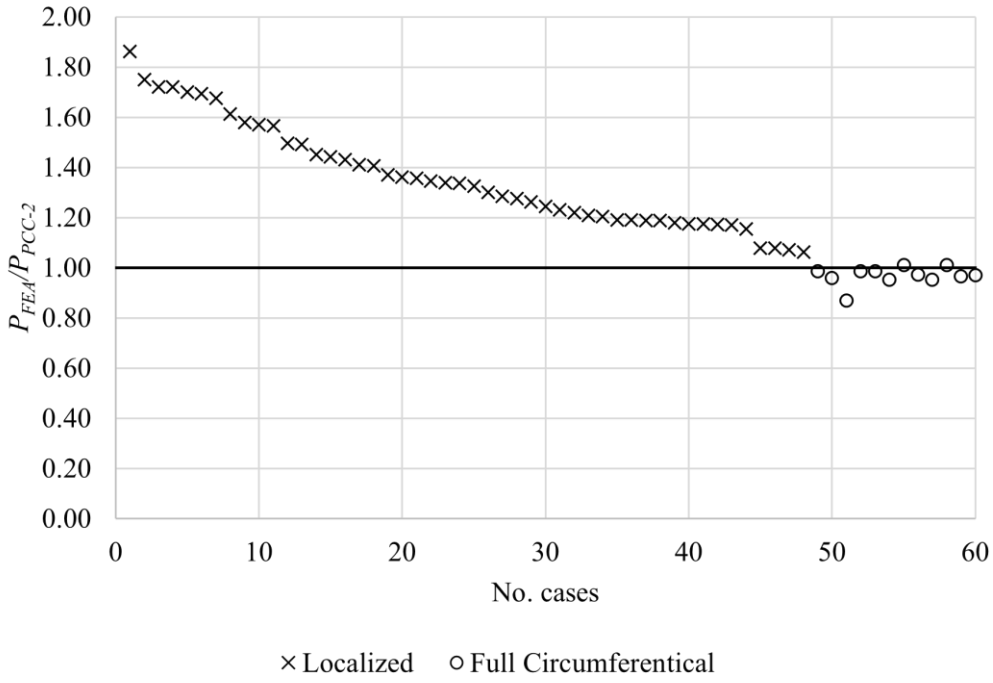

Figure 2.9 Accuracy of ASME PCC-2 equation to predict burst capacity for localized and full-circumferential defects

Table 2.5 Mean and COV of P_{FEA}/P_{PCC-2} for the 60 FEA cases

		Localized defects (48 cases)	**Full circumferential defects (12 cases)**
P_{FEA}/P_{PCC-2}	Mean	1.46	0.97
	COV	0.39	0.04

Equation (2.10) is further applied to the 9 full-scale tests that are included in Table 2.4 and failed on the FRP repair (i.e. excluding those that failed on the substrate). The results are shown in Table 6, which clearly indicates that Eq. (2.10) is inadequate for localized defects.

Table 2.6 Accuracy of the PCC-2 model in comparison with the full-scale tests

		Localized defects
P_{test}/P_{PCC-2}	Mean	1.43
	COV	0.86

2.4.3 Defect width correction factor

Given the results shown in Fig. 2.9 and Table 2.5, a defect width correction factor (f_w) is proposed for $P_{PCC\text{-}2}$ to improve its predictive accuracy for the localized corrosion defect. The results presented in Section 2.3 indicate that P_w/P_{circ} depends on the normalized defect depth, length and width. The following empirical equation is developed to compute f_w based on nonlinear regression analyses of the P_w/P_{circ} ratios obtained from the parametric FEA cases:

$$f_w = [(1.05 - 0.6\,d') + (0.01(w'L')^{0.35})]\left(\frac{1+0.0005(1-d')L'^2}{(w')^{0.05}}\right) \quad (2.11)$$

The presented correction factor is applicable to CRC pipelines containing localized defects with $0.3 \leq d' \leq 0.7$, $0.5 \leq L' \leq 20$, and $0.5 \leq w' \leq 20$, and repaired with unidirectional glass fibre. Figure 2.10 shows that Eq. (2.11) fits well the values of P_w/P_{circ} for the 48 parametric FEA cases with localized defects.

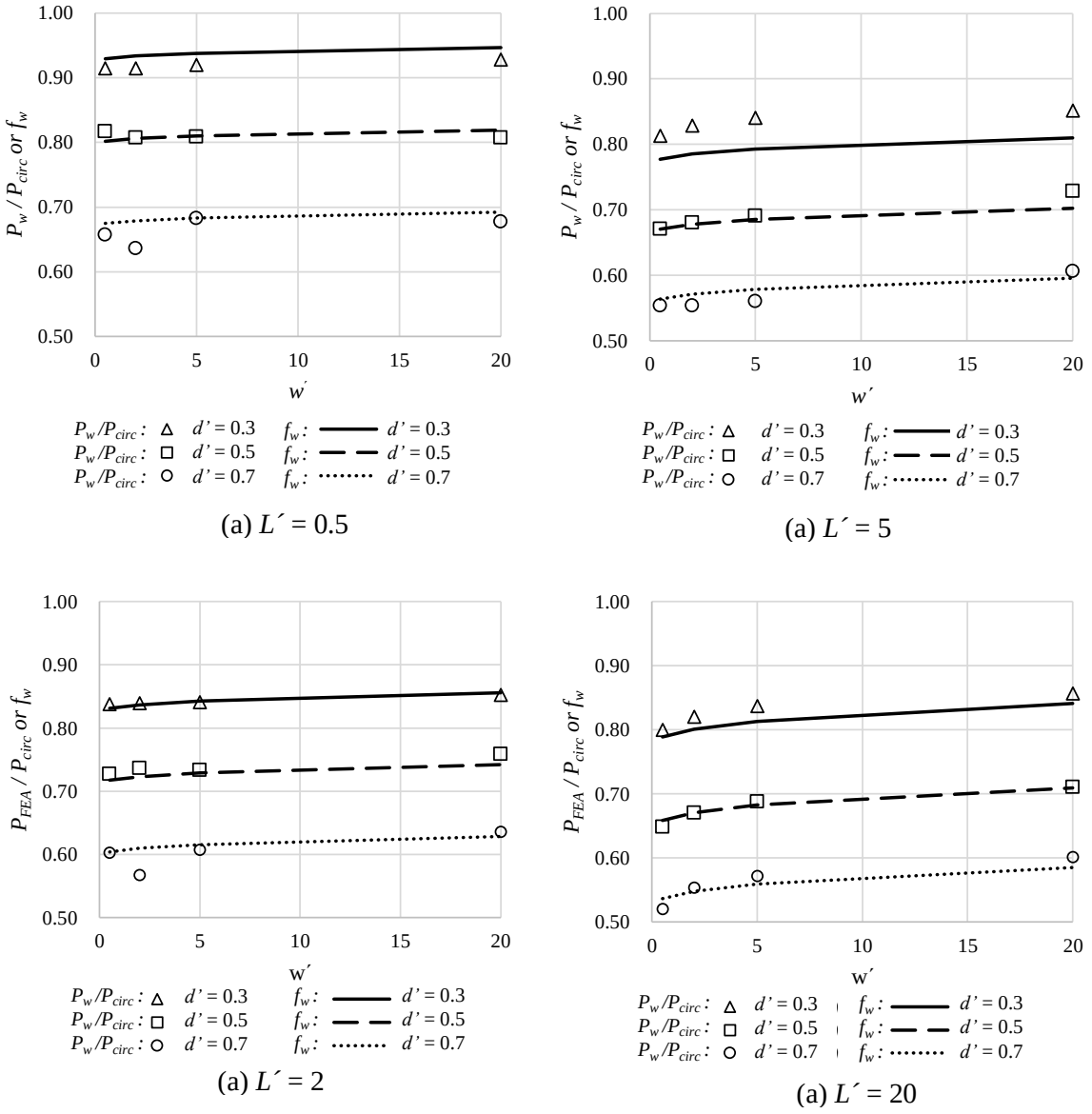

Figure 2.10 Predicted and FEA results of width effect on burst capacity of localized defects

A new burst capacity model, $P_{PCC2\text{-}w}$, is then proposed by incorporating the defect width correction factor; that is, $P_{PCC2\text{-}w} = f_w P_{PCC\text{-}2}$, where f_w is given by Eq. (2.11). The mean and COV of $P_{FEA}/P_{PCC2\text{-}w}$ for the 48 parametric FEA cases are summarized in Table 2.7. Furthermore, P_{FEA} are compared with $P_{PCC2\text{-}w}$ and P_{PCC2} for the 60 parametric cases in Fig. 2.11. The results in Table 2.7 and Fig. 2.11 show that the predictive accuracy of the PCC2-*w* model is markedly higher than that of the PCC-2 model.

Table 2.7 Comparison of the predictive accuracy of the PCC-2 and PCC2-w models for the 60 parametric FEA cases

	P_{FEA}/P_{PCC-2}	P_{FEA}/P_{PCC2-w}
Mean	1.46	0.97
COV	0.39	0.14

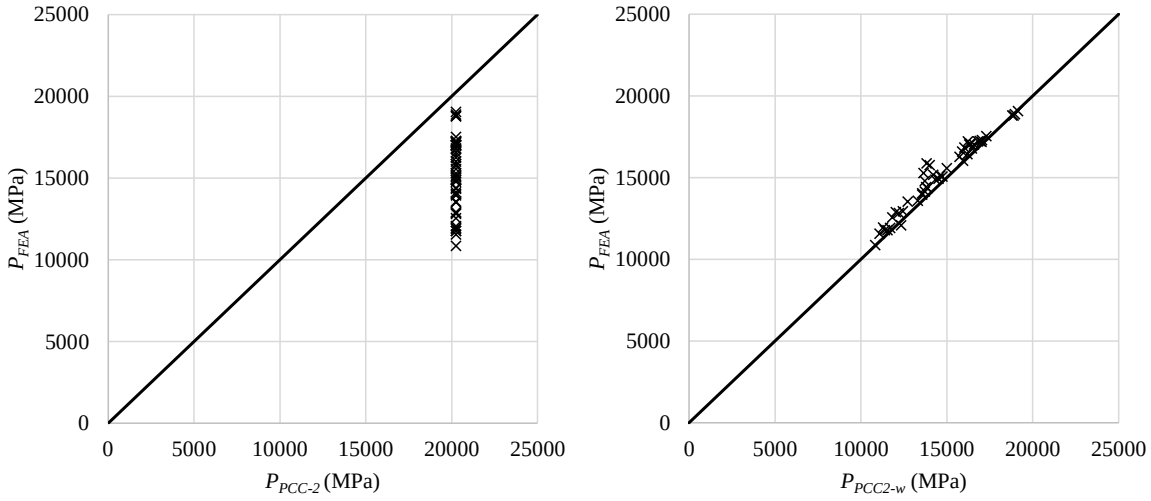

(a) Accuracy of PCC-2 model (b) Accuracy of PCC2-w model

Figure 2.11 Comparison of PPCC-2 with PFEA and PPCC2-w with PFEA for the 60 parametric FEA cases

2.5 Conclusions

In this chapter, parametric FEA is carried out to investigate the effect of the corrosion defect width on the burst capacity of CRC pipelines. Full-scale burst tests of CRC pipe specimens reported in the literature are used to validate the finite element model. The analysis results indicate that the burst capacity of a CRC pipeline with a localized corrosion defect is markedly lower than that of a CRC pipeline with a full-circumferential defect of the same depth and length. The reduction in the burst capacity is greater for deeper defects. The reduction is due to the significant bulging response under internal pressure for pipelines containing localized corrosion defect.

The burst capacity model derived from the design equation recommended in the ASME PCC-2 code is found to be markedly non-conservative for CRC pipelines containing localized corrosion defects based on a comparison with results from the parametric FEA. An empirical equation for the defect width correction factor is then developed from non-linear regression analyses and applied to the prediction by the PCC-2 model. It is demonstrated that the predictive accuracy of the PCC-2 model after the application of the width correction factor is markedly improved.

References

[1] F.G. Alabtah, E. Mahdi, F.F. Eliyan. The use of fibre reinforced polymeric composites in pipelines: a review. Composite Structures 276 (2021) 114595

[2] K.S. Lim, S. Azraai, N. Yahaya, M. Noor, L. Zardasti, JHJ. Kim. Behaviour of steel pipelines with composite repairs analyzed using experimental and numerical approaches. Thin-Walled Struct. 139 (2019) 321–33

[3] J. Duell, J. Wilson, M. Kessler. Analysis of a carbon composite overwrap pipeline repair system. The International journal of Pressure Vessels and Piping 85(11) (2008) 728-788

[4] American Society of Mechanical Engineers. Non Metallic and Bonded Repairs. In ASME PCC-2-2018 Repair of Pressure Equipment and Piping: An American national standard (2018)

[5] International Standard Organization. ISO-24817 Petroleum, petrochemical and natural gas industries: composite repairs for pipework: Qualification and design, installation, testing and inspection (2017)

[6] H. da Costa Mattos, J.M. Reis, M. Da Silva, F. Amorim, V. Perrut. Analysis of a glass fibre reinforced polyurethane composite repair system for corroded pipelines at elevated temperatures. Composite structures 114 (2014) 117-123

[7] P.H. Chan, K.Y. Tshai, M. Johnson, L.H. Choo, S. Li, K. Zakaria. Burst strength of carbon fibre reinforced polyethylene strip pipeline repair system – a numerical and experimental approach. Journal of Composite Materials 49(6) (2015) 749-756

[8] A. Ali, M. Zahiraniza, M. Thar. Burst capacity of pipe under corrosion defects and repaired with thermosetting liner. Steel and composite structures 35(2) (2020) 171-186

[9] J. Chen, H. Wang, M. Salemi, P.N. Balaguru. Finite element analysis of composite repair for damaged steel pipeline. Coatings 11(3) (2021) 301

[10] D. Kong, X. Huang, M. Xin, G. Xian. Effects of defect dimensions and putty properties on the burst performances of steel pipes wrapped with CFRP composites. The International Journal of Pressure Vessels and Piping 186 (2020) 104-139

[11] W. Zhou, G.X. Huang. Model error assessments of burst capacity models for corroded pipelines. The international journal of Pressure Vessels and Piping 99-100 (2012) 1-8

[12] S. Zhang, W. Zhou. Assessment of effects of idealized defect shape and width on the burst capacity of corroded pipelines. Thin-walled structures 154 (2020) 106806

[13] L. Meniconi, J. Freire, R. Vieira, J. Diniz. Stress analisis of pipelines with composite repairs. Proceedings of the 2002 4th International Pipeline Conference (2002) 2031-2037

[14] F. Al Abtah, E. Mahdi, S. Gowid. The use of composite to eliminate the effect of welding on the bending behaviour of metallic pipes. Composite structures 235 (2020) 111793

[15] X.K. Zhu, B.N. Leis. Influence of the yield-to-tensile strength ratio on failure assessment of corroded pipelines. Journal of pressure vessel technology 127(4) (2005) 436-442

[16] Dowling, N. E. (2007) Mechanical behavior of materials : engineering methods for deformation, fracture and fatigue. 3rd ed. Upper Saddle River, NJ: Pearson Prentice Hall.

[17] Z. Hashin. Failure criterion for unidirectional fiber composites. Journal of applied mechanics 47(2) (1980) 329-334

[18] R. Her, J. Renard, V. Gaffard, Y. Favry, P. Wiet. Design of pipeline composite repairs: from lab scale tests to FEA and full-scale testing. Proceedings of the 2014 10th international pipeline conference Vol.2 (2014)

[19] L. Mazurkiewicz, M. Tomaszewski, J. Malachowski, K. Sybilski, M. Chebakov, M. Dimitrenko. Experimental and numerical study of steel pipe with part-wall defect reinforced with fibre glass sleeve. The International Journal of Pressure Vessels and Piping 149 (2017) 108-119

[20] S. Ahankari, A. Patil. Sea water effect on mechanical performance of steel pipes rehabilitated with glass fiber reinforced epoxy composites. Materials today: Proceedings 22 (2020) 2490-2498

[21] R.T. Ferreira, I.A. Ashcroft. Optimal orientation of fiber composites for strength based on Hashin's criteria optimality conditions. Structural and multidisciplinary optimization 61(5) (2020) 2155-2176

Chapter 3

3 Development of an enhanced model to predict the burst capacity of composite repaired corroded pipelines using Gaussian process regression

3.1 Introduction

Oil and gas pipelines play a crucial role in the transportation of energy resources worldwide. Corrosion is a significant threat to the integrity and can lead to leaks and ruptures of pipelines. Composite repair systems have been developed to repair and reinforce corroded pipelines. However, predicting the burst capacity of composite repaired corroded (CRC) pipelines is challenging due to the complexity of composite materials and the different defect dimensions, especially when high elastic modulus materials such as carbon fibre are incorporated. Existing prediction models and design equations often fail to account for these complexities and can result in inaccurate burst capacity predictions [1, 2, 3].

The rehabilitation of corroded pipelines using composite materials consists of placing the composite material in layers over the external wall of the corroded section of the pipe. The composite material used in this application is fibre reinforced polymer (FRP), which consists of fibre reinforcements (i.e. fiberglass or carbon fibre) in a polymer matrix. This type of repair provides a durable, corrosion resistant and economical solution to extend the service life of pipelines. The required thickness (th_{repair}) and length (L_{repair}) of the composite can be determined using standards such as ISO 24817 [4] and ASME PCC-2 [5]. The ASME PCC-2 design code includes an equation to calculate the minimum thickness of a composite repair. This equation can be recast to calculate the maximum pressure (i.e. burst capacity) that can be resisted for a given repair thickness. According to some studies [1, 6], these codes result in conservative designs for certain cases. On the other hand, Da Mattos et al [6] showed that they can also lead to over-prediction of the burst capacity of the CRC pipeline.

The objective of this study is to investigate the parameters that affect the accuracy of the ASME PCC-2 equation for predicting the burst capacity of CRC pipelines and to develop

a correction factor that accounts for such effects. This is achieved by incorporating a correction term estimated using a machine learning model, Gaussian Process Regression (GPR), and burst capacities obtained from extensive parametric finite element analyses (FEA).

FEA has been employed to predict the burst capacity of CRC pipelines and shown to be accurate when compared with results of full-scale burst tests [6, 8, 9, 10]. Since there is not enough data from full scale tests available in existing literature to use as a training set for GPR, the full-scale tests are used to validate the FEA model, and an extensive parametric analysis involving a large number of analysis cases is carried out. The results of 864 FEA cases are used to train and test the GPR model.

The rest of the paper is organized as follows. Section 2 describes the FEA model used in this study and its validation using full-scale tests collected from literature. Section 3 presents the parametric analysis cases and compares the burst capacities of these cases predicted using FEA and the burst capacity model derived from the ASME PCC-2 design code. The application of GPR is described in Section 4. The GPR model is built using a squared exponential kernel and a zero-mean function with seven input variables based on the input and the observed results from the parametric analysis. We present the results of the model and the improvement achieved on the test set for validation. Section 5 presents concluding remarks.

3.2 FEA model

3.2.1 General

The FEA model of a CRC pipeline has three components: the corroded steel pipeline section (hereafter called the substrate), the putty that fills the defect void, and the FRP repair. The commercial package Abaqus 2020 is used to develop models of CRC pipelines and simulate their responses under internal pressure until failure is reached. Figs. 3.1(a) and 3.1(b) show the three components of the CRC pipeline modelled in Abaqus. The substrate, FRP and putty are shown in red, green, yellow, respectively. Fig. 3.1(c) depicts the model on Abaqus of a CRC pipeline with the putty placed on the void of the defect and the composite wrapped around the defect.

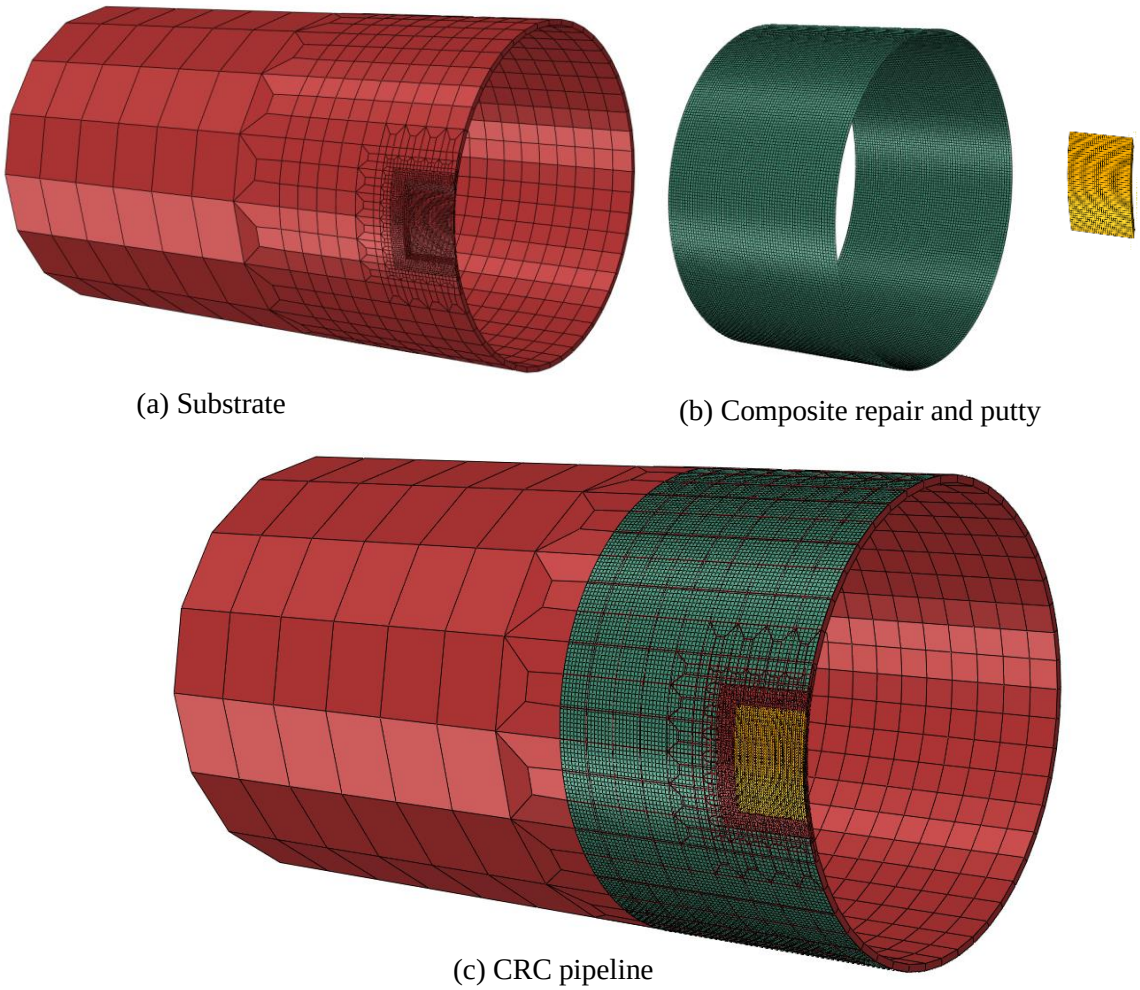

(a) Substrate

(b) Composite repair and putty

(c) CRC pipeline

Figure 3.1 Abaqus model of a CRC pipeline

The validity of the FEA model has been verified in the previous chapter using 11 cases of full-scale tests of CRC pipelines reported in the literature.

3.2.2 Model Specifics

The steel is modelled as an isotropic material using the C3D8R solid element (i.e. the 8-node linear brick element with reduced integration points). The true stress (σ) – true strain (ε) relationship of the steel is assumed to be as follows [11]:

$$\sigma = E\,\varepsilon \quad \sigma < \sigma_y \tag{3.1}$$

$$\sigma = K\varepsilon^n \quad \sigma \geq \sigma_y \tag{3.2}$$

where E is Young's modulus; σ_y denotes the yield strength, and K and n are the coefficients of the power-law stress-strain relationship in the plastic domain and can be determined from the coupon tensile test data. If such test data are unavailable, n can be estimated using the following empirical equation proposed in [12].

$$n = 0.239\left(\frac{1}{\sigma_y/\sigma'_{uts}} - 1\right)^{0.596} \tag{3.3}$$

where σ'_{uts} is the ultimate tensile strength. Finally, Eq. (3.4), which is derived based on Considere´s criterion [13], can be used to calculate K.

$$K = \frac{e^n}{n^n}\sigma'_{uts} \tag{3.4}$$

Many polymeric materials with high compression strengths are suitable choices for putty. In this study, putty is characterized as an isotropic elastic material and modelled using the C3D8R element. The properties required for modelling the putty are its elastic modulus (E_p) and Poisson's ratio (v_p). A parametric study reported in [10] indicates that the elastic modulus of the putty has a minor effect on the burst capacity of the CRC pipeline.

The composite material or FRP includes a polymer matrix that binds the fibre (reinforcement). Mechanical properties of the composite material can be obtained by performing mechanical tests on specimens made with the same materials, thickness layers, composition (%) and angle of orientation of the reinforcement. The composite sleeve is modelled using the S4R (4-node curved shell element with reduced integration) elements in Abaqus. It is assigned with a composite layup to define the thickness and properties of each ply. The global axis of the model are defined as X, Y and Z, and the local coordinates for the composite layup are defined as 1,2 and 3 on the shell element in Abaqus. Where the local axis 1 is in the hoop direction of the pipe (longitudinal direction of the FRP repair), the local axis 2 is in the axial direction of the pipe (transverse direction of the FRP repair) and local axis is in the direction normal to the shell element.

Since the composite material has reinforcement in a specific direction (i.e. in axis 1), it is considered an orthotropic elastic material with the plane stress condition. This is defined

in Abaqus as *Lamina*. The corresponding stress-strain relationship is given by Eq. (3.5) [8], where ε_{ij} and σ_{ij} denote the strains and stresses in the local coordinate system of the composite (i, j = 1, 2).

$$\begin{Bmatrix}\varepsilon_{11}\\ \varepsilon_{22}\\ \varepsilon_{12}\end{Bmatrix} = \begin{bmatrix} 1/E_1 & -\nu_{12}/E_1 & 0 \\ -\nu_{12}/E_1 & 1/E_2 & 0 \\ 0 & 0 & 1/G_{12}\end{bmatrix}\begin{Bmatrix}\sigma_{11}\\ \sigma_{22}\\ \tau_{12}\end{Bmatrix} \tag{3.5}$$

The material stability for the plane stress condition requires that:

$$|\nu_{12}| < (E_1/E_2)^{1/2} \tag{3.6}$$

Different criteria have been proposed in the literature to define failure of CRC pipelines in FEA. In general, the failure criterion considers failures of the steel substrate and FRP repair. For the substrate, failure is defined as the point at which the maximum nodal von Mises true stress within the corrosion defect region reaches the true stress corresponding to the ultimate tensile strength [11]. For FRP, the Tsai-Wu [14] and Hashin [15] damage criteria are the most used in the literature.

The Hashin criterion is considered in this study because it is more advantageous than the Tsai-Wu criterion since the former is based on a system of equations and considers the failure on both the matrix and the fibre, while the latter is based on a single failure mode. Furthermore, the Hashin criterion is a built-in option in Abaqus. Four damage indices are included in the Hashin criterion, i.e. FTCRT, FCCRT, MTCRT and MCCRT, corresponding to the fibre tension, fibre compression, matrix tension and matrix compression failures, respectively. For CRC pipelines, only FTCRT and MTCRT, i.e. fibre and matrix tension failures, are relevant. These two indices are calculated as follows: using the tensile and shear stresses obtained from FEA and the material resistances in three directions: X_T (longitudinal tensile strength), Y_T (transverse tensile strength) and S_L (longitudinal shear strength).

$$\text{FTCRT}= \left(\frac{\hat{\sigma}_{11}}{X_T}\right)^2 + \alpha\left(\frac{\hat{\tau}_{12}}{S_L}\right)^2 \tag{3.7}$$

$$\text{MTCRT}= \left(\frac{\hat{\sigma}_{22}}{Y_T}\right)^2 + \left(\frac{\hat{\tau}_{12}}{S_L}\right)^2 \tag{3.8}$$

where $\hat{\sigma}_{11}$ (≥ 0), $\hat{\sigma}_{22}$, (≥ 0) and $\hat{\tau}_{12}$ are components of the effective stress tensor; α is a coefficient that determines the contribution of the shear stress; X_T, Y_T and S_L are the longitudinal tensile strength, transverse tensile strength, and longitudinal shear strength of FRP, respectively. If either FTCRT or MTCRT reaches unity, failure of the composite is reached. The values of $\hat{\sigma}_{11}$, $\hat{\sigma}_{22}$, and $\hat{\tau}_{12}$ are calculated by multiplying the corresponding stress tensor components (i.e. σ_{11}, σ_{22} and σ_{12}) with a damage factor [15]. Prior to any damage it can be assumed that $\hat{\sigma} = \sigma$ [19], which is consistent with the analysis carried out in the present study as the analysis ends once damage is initiated. Hashin pointed out that Eq. (3.7) can be simplified with an adequate accuracy by assuming α = 0, which results in FTCRT being defined by,

$$\text{FTCRT}= \left(\frac{\hat{\sigma}_{11}}{X_T}\right)^2 \tag{3.9}$$

It follows that failure will occur if $\hat{\sigma}_{11}$ equals X_T. Opposed to matrix failure modes that go parallel to the direction of the fibre. Fibre failure modes corresponds to failure of the FRP on the direction of the reinforcement, these can be identified when the rupture goes through the fibre.

3.3 Burst capacity model and parametric FEA

3.3.1 ASME PCC-2 model

In part 4 of the ASME PCC-2 code [5], two approaches are provided to calculate the minimum thickness of the FRP repair for CRC pipelines. The first one is provided for designs where the substrate is expected to yield, while the second one focuses on cases where yielding is not expected. This study focuses on the first approach, which is the most common scenario and used equation in the literature. This method considers that the defect depth (d) is the only known defect dimension and that the substrate behaves in an elastic-perfectly plastic manner, yielding when the burst capacity of the CRC pipe is reached. To

apply the first approach, the burst capacity prediction equation based on the ASME PCC-2 code can be recast as follows:

$$P_{PCC-2} = \frac{2}{D}\left(th_{repair}X_T + \sigma_y t_{s'}\right) \tag{3.10}$$

where t_s represents the remaining thickness of the substrate material on the defect area, (i.e. $t_{s'} = t - d$). Equation (3.10) is derived based on the well-known Barlow equation, which is commonly used to calculate the burst pressure of pipes. However, in this case, the equation is extended by considering the contributions of both the composite and the substrate to withstand the pressure. The term $th_{repair}X_T$ accounts for the contribution of the FRP repair to the burst capacity, and the term $\sigma_y t_{s'}$ accounts for the capacity of the substrate.

3.3.2 Parametric analysis cases

The dimensions and properties of the pipelines as well as the repair dimensions and material properties of the cases considered in the parametric analysis are summarized in this section. These are representative of specimens found in full-scale tests documented in the literature, as well as those of in-service oil and gas transmission pipelines.

For the analysis, a pipe model with an outside diameter (D) of 457 mm, a thickness (t) of 7.11 mm, and a steel grade of X60 is used. The assumed yield strength (σ_y) is 455 MPa. Two yield to tensile strength ratios (σ_y/σ'_{uts}) are considered: 0.8 and 0.765. The coefficients of the stress-strain relationship in the plastic domain, K and n, were estimated using Eqs. (3) and (4) corresponding to the two yield to tensile strength ratios. The composite repair material is assumed to be an epoxy polymer with fiberglass reinforcement. The elastic modulus in the hoop direction of the composite material (E_1) is assumed to be 0.05E, 0.2E, and 0.5E (i.e. 10.5, 42, and 105 GPa), and the elastic modulus in the axial direction (E_2) is 1.05, 4.2 and 10.5 GPa, based on information in the literature [3,6,7,8] for unidirectional fibre composite repairs. Failure of the composite in the hoop direction is assumed to occur at a hoop strain (ε_{hc}) of 0.01 [6, 19]. Consequently, the tensile strength in the hoop direction ($X_T = \varepsilon_{hc}E_1$) is 105, 420 and 150 MPa, respectively for every corresponding value of the elastic modulus. The Hashin resistances of unidirectional fiber-reinforced composite

materials for glass-epoxy, as reported in [20], are adopted (i.e. Y_T and S_L are assumed as 35 and 72 MPa, respectively).

The repair thickness (th_{repair}) was calculated as 0.5, 1, and 1.5 times the ASME PCC-2 design calculated repair thickness of the pristine pipe section th_{pcc2} for a pressure equal to the predicted capacity (i.e. $P_{PCC\text{-}2}$ = 20 MPa). The putty used has an elastic modulus (E_p) of 2400 MPa and a Poisson's ratio (v_p) of 0.28 [19]. Let d, L and w denote the depth (in the through wall thickness direction), length (in the pipe longitudinal direction) and width (in the pipe circumferential direction) of the corrosion defect, respectively. The normalized depths of the defect ($d' = d/t$) considered are 0.3, 0.5, and 0.7. The normalized defect lengths ($L' = L^2/(Dt)$) and normalized defect widths ($w' = w^2/(Dt)$) are set to 0.5, 2, 5, and 20. This results in a total of 48 defect dimensions. With the different properties of the pipe steel and composite repair, there are a total of 864 analysis cases considered in the parametric FEA.

3.3.3 Observations from parametric FEA

The burst capacities of the 864 parametric analysis cases described in the previous section are computed using FEA and used as the benchmark to evaluate the accuracy of Eq. (3.12) (referred to as the PCC-2 model hereafter). Figure 3.1 compares the burst capacities predicted by the PCC-2 model ($P_{PCC\text{-}2}$) and FEA (P_{FEA}). Figs. 3.1(a), 3.1(b) and 3.1(c) show the results for E_1 equal to 0.05E, 0.2E and 0.5E, respectively. The figure indicates that the higher E_1, the greater is the degree of inaccuracy of the PCC-2 model.

The mean value of $P_{PCC\text{-}2}/P_{FEA}$ for the 864 cases is 1.52, and the coefficient of variation (COV) equals 0.48. This indicates that the PCC-2 model in general markedly overestimates the burst capacity of CRC pipelines. Fig. 3.1(a) suggests that for cases with low elastic modulus (and low X_T), failure occurs only along the longitudinal direction of the repair (i.e. failure mode: HSNFTCRT). For cases with higher elastic modulus, such as those shown in Fig. 1(b) and especially Fig. 3.1(c), both failure modes on the composite repair occur, including HSNFTCRT and failure due to tension on the matrix (i.e. HSNMTCRT). These results suggest that the accurate prediction of the burst capacity of CRC pipelines can be a sophisticated process.

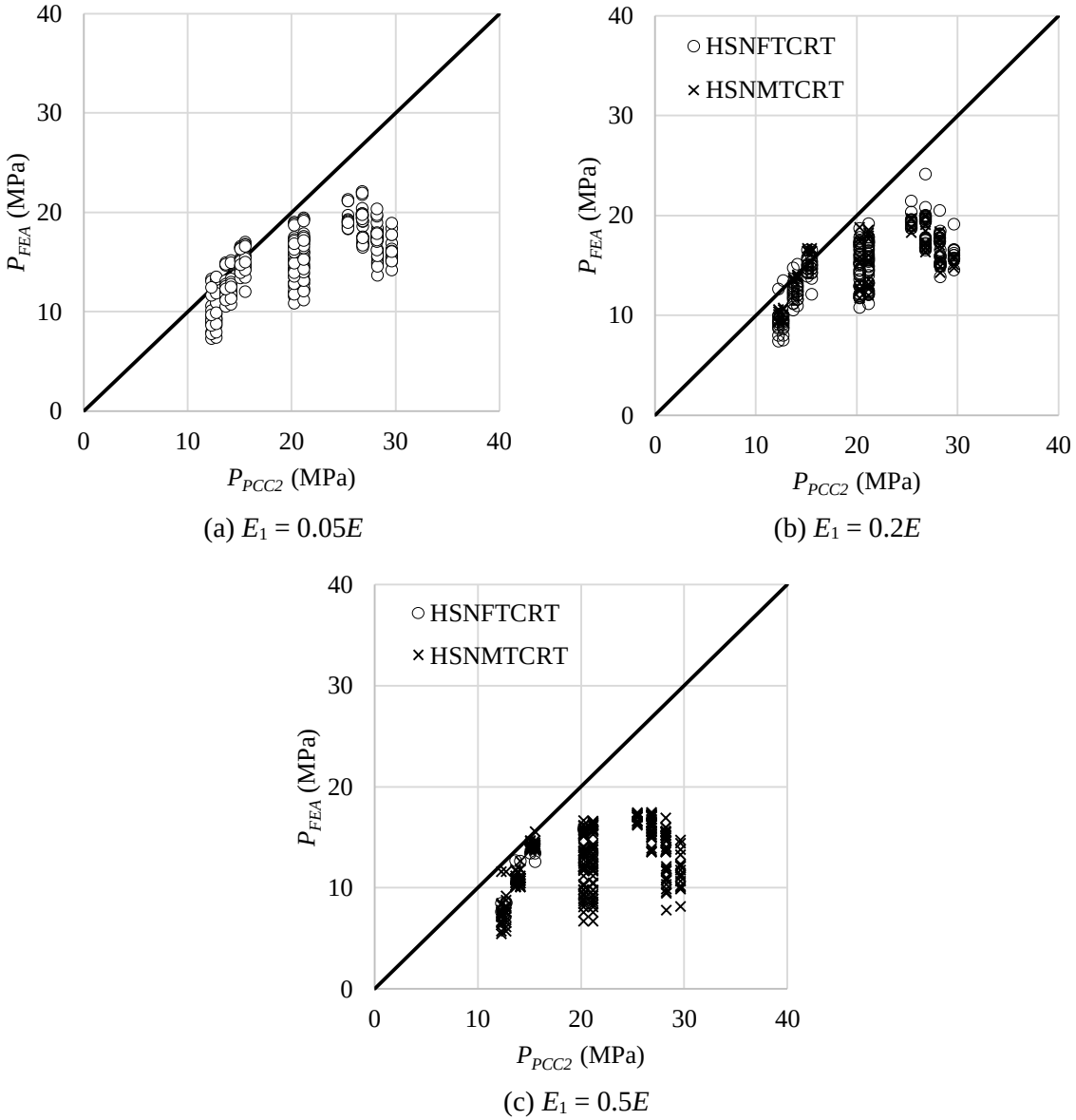

(a) $E_1 = 0.05E$ (b) $E_1 = 0.2E$

(c) $E_1 = 0.5E$

Figure 3.2 Accuracy of the PCC-2 model for different elastic modulus

To improve the PCC-2 model accuracy to predict the burst capacity of CRC pipelines, the GPR model is set to predict the ratio $P_{PCC\text{-}2}/P_{FEA}$ (that represents the error or *correction* needed on the prediction when we take the FEA-predicted burst capacity as benchmark). For this purpose, it uses the input variables described on Section 3.4 and the $P_{PCC\text{-}2}/P_{FEA}$ ratio on each case to predict the correction factor (f_{GPR}) for the regression set. The correction factor, which accounts for the seven input variables that correlate to the burst capacity of the pipe and are not included on the PCC-2 equation, is incorporated in the

existing PCC-2 model to propose a new model based on the results of the GPR (P_{GPR}), expressed as:

$$P_{GPR} = P_{PCC-2}\,(1/f_{GPR}) \tag{3.11}$$

3.4 Gaussian process regression

3.4.1 General

The following section provides an overview of Gaussian process regression (GPR), focusing on the squared exponential kernel with a zero-prior mean, and its potential in predicting a correction factor to improve the accuracy of the PCC-2 model.

In GPR, we consider a set of input variables represented by the vector $\mathbf{x} = \{x_1, x_2, \ldots, x_s\}$ where s represents the number of input variables (7 in this case). Eq. (3.14) shows the 7 input variables selected for this analysis; these are normalized to improve the model performance avoiding using different units. The scalar output, denoted as Y, is a function of the 7-dimensional vector of input variables. [21]

$$\mathbf{x_i} = \{x_{i1}, x_{i2}, x_{i3}, x_{i4}, x_{i5}, x_{i6}, x_{i7}\} = \left\{\frac{d}{t}, \frac{L^2}{Dt}, \frac{w^2}{Dt}, \frac{t_{repair}}{t_{pcc}}, \frac{E_c}{E}, \frac{Y}{T}, \frac{Y_T}{X_T}\right\} \tag{3.12}$$

$$\mathbf{Y} = \{Y(\mathbf{x}_1), Y(\mathbf{x}_2), \ldots, Y(\mathbf{x}_n)\} \tag{3.13}$$

where n represents the number of cases, i and j are used for the different input cases or "rows" of data, in this case up to 70% of 864 = 605 different cases randomly selected for training). The input variables were selected based on the information that was considered to be correlated to the burst capacity of the CRC pipelines and that wasn't considered on the PCC-2 model. On the GPR model, the hyperparameters were estimated to increase the maximum likelihood, to give more weight to those input variables who had a bigger effect on the correction factor predicted.

The set of output values $\mathbf{Y}$ follows a Gaussian process, with its distribution expressed as $\mathbf{Y} \sim N(\boldsymbol{\mu}, \boldsymbol{\Sigma})$, where $\boldsymbol{\mu}$ represents the mean vector and $\boldsymbol{\Sigma}$ represents the covariance matrix. The mean function represents the expected value of $\mathbf{Y}$ at each input value, while the covariance

function represents the degree of similarity between the response values at different input values. A prior mean ($\boldsymbol{\mu}$) of zero is considered as is often assumed in the literature [24]; this means that the mean function of the GPR model is set to zero for all input data points before updating is carried out based on observations. Therefore, $\mathbf{Y}$ can be represented as ~ N($\mathbf{0}$, $\boldsymbol{\Sigma}$) [22]. The GPR model then attempts to predict the response values at new input values. It achieves this by calculating the conditional distribution of $\mathbf{Y}$ given the observed data. Importantly, this conditional distribution is also a Gaussian distribution, with a mean and covariance that are influenced by the observed data and the kernel function.

The covariance between $Y(\mathbf{x}_i)$ and $Y(\mathbf{x}_j)$, denoted as σ_{ij} ($i, j = 1, 2, \ldots, n$), is evaluated as $\sigma_{ij} = k(\mathbf{x}_i, \mathbf{x}_j)$, where $k(\mathbf{x}_i, \mathbf{x}_j)$ is a suitably chosen covariance function or kernel of $\mathbf{x}_i$ and $\mathbf{x}_j$ [23]. Essentially, σ_{ij} represents the covariance between the output values at two different input locations; $Y(\mathbf{x}_i)$ and $Y(\mathbf{x}_j)$. To construct the covariance matrix $\boldsymbol{\Sigma}$, one utilizes the covariance values obtained from applying the kernel to each pair of input points. The covariance matrix is then defined as:

$$\boldsymbol{\Sigma} = \begin{matrix} [k(\mathbf{x}_1, \mathbf{x}_1), k(\mathbf{x}_1, \mathbf{x}_2), \ldots, k(\mathbf{x}_1, \mathbf{x}_n)] \\ [k(\mathbf{x}_2, \mathbf{x}_1), k(\mathbf{x}_2, \mathbf{x}_2), \ldots, k(\mathbf{x}_2, \mathbf{x}_n)] \\ \ldots \\ [k(\mathbf{x}_n, \mathbf{x}_1), k(\mathbf{x}_n, \mathbf{x}_2), \ldots, k(\mathbf{x}_n, \mathbf{x}_n)] \end{matrix} \tag{3.14}$$

Radial basis function or squared exponential kernel (k_{SE} hereafter) function is often used in the literature and also adopted in the present study. This particular kernel measures the similarity based on the distance between two data points. If two points are very close together, they will have high similarity. In other words, the kernel function is a measure of the similarity or correlation between the outputs $Y(\mathbf{x}_i)$ and $Y(\mathbf{x}_j)$ based on the similarity between the inputs $\boldsymbol{x}_i$ and $\boldsymbol{x}_j$ [24]. Mathematically, it is defined as:

$$k_{SE}(\mathbf{x}_i, \mathbf{x}_j) = \eta_y^2 \exp\left(-\frac{1}{2} \sum_{q=1}^{s} \frac{(x_{iq} - x_{jq})^2}{l_q^2} \right) \tag{3.15}$$

where $\boldsymbol{x}_i$ and $\boldsymbol{x}_j$ are the input data points and represent the entire input vectors for two different cases i and j, respectively. η_y^2 represents the variance of the GPR and is a

hyperparameter that controls the level of fluctuation in the output of the model. It represents the uncertainty in the relationship between the input variables and the output variable. $\|\boldsymbol{x}_i - \boldsymbol{x}_j\|$ is the Euclidean distance between the data points, and the length scale l_q (q = 1, 2, …, s) is a hyperparameter that controls the smoothness of the equation [24]. It characterizes the relevance of x_q. The greater is l_q, the less relevant is x_q in GPR.

If $\boldsymbol{x}_i$ and $\boldsymbol{x}_j$ are "nearby" in the input space, then $\mathbf{Y}_i$ and $\mathbf{Y}_j$ have a high covariance. If $\boldsymbol{x}_i$ and $\boldsymbol{x}_j$ are "far away" in the input space, then $\mathbf{Y}_i$ and $\mathbf{Y}_j$ have a low covariance.

Let $\mathbf{Y}$ be then divided into two disjoint subsets: $\mathbf{Y}_t$ (training) and $\mathbf{Y}_r$ (regression) of dimensions m and (n – m), respectively. If noisy values of $\mathbf{Y}_t$, $\mathbf{z}_t$, have been observed, it follows from the property of the joint Gaussian distribution that the distribution of $\mathbf{Y}_r$ conditional on $\mathbf{z}_t$ is also Gaussian and expressed as [21],

$$\mathbf{Y}_r|\mathbf{z}_t \sim \mathrm{N}(\boldsymbol{\mu}_{r|t}, \boldsymbol{\Sigma}_{r|t}) \tag{3.16}$$

$$\boldsymbol{\mu}_{r|t_n} = \boldsymbol{\Sigma}_{rt}(\boldsymbol{\Sigma}_t + \eta_n^2\mathbf{I})^{-1}(\boldsymbol{z}_t) \tag{3.17}$$

$$\boldsymbol{\Sigma}_{r|t_n} = \boldsymbol{\Sigma}_r - \boldsymbol{\Sigma}_{rt}(\boldsymbol{\Sigma}_t + \eta_n^2\mathbf{I})^{-1}(\boldsymbol{\Sigma}_{rt})^{\mathrm{T}} \tag{3.18}$$

where $\boldsymbol{\Sigma}_t$ and $\boldsymbol{\Sigma}_r$ are the (prior) covariance matrices of $\mathbf{Y}_t$ and $\mathbf{Y}_r$, respectively; $\boldsymbol{\Sigma}_{rt}$ is the (n-m) × m covariance matrix between the elements of $\mathbf{Y}_r$ and those of $\mathbf{Y}_t$; "T" denotes transposition; and $\boldsymbol{\mu}_{r|t}$ and $\boldsymbol{\Sigma}_{r|t}$ are the mean and covariance of $\mathbf{Y}_r$ conditional on $\mathbf{z}_t$ (i.e. the posterior mean and covariance); $\mathbf{I}$ is the identity matrix with the same size as $\boldsymbol{\Sigma}$, and η_n^2 is the variance of the noise [21]. It follows from Eqs. (3.16) to (3.18) that the mean and covariance of $\mathbf{Y}_r$ are updated based on observed noisy values of $\mathbf{Y}_t$. In the above formulations, it is assumed that the noise included in the observation of $\mathbf{Y}_t$ is independent, identically Gaussian distributed with a zero mean and a variance of η_n^2.

In the GPR model, the hyperparameters of the kernel function, such as σ and l_q (q = 1, 2, …, 7), are optimized through maximum likelihood estimation during the training process. The resulting GPR model can then be used to make predictions on new input data by using

the covariance matrix between the new data points and the training data points. In the case of a squared exponential kernel function and a zero prior mean, the log-likelihood can be expressed as shown in Eq. (3.18) [21].

$$\ln\big(L(\boldsymbol{\theta}|\mathbf{z}_t)\big) = -\tfrac{1}{2}(\mathbf{z}_t)^{\mathrm{T}}(\boldsymbol{\Sigma}_t + \sigma_n^2\mathbf{I})^{-\mathbf{1}}(\mathbf{z}_t) - \tfrac{1}{2}\ln(\det(\boldsymbol{\Sigma}_t + \sigma_n^2\mathbf{I})) - \tfrac{\mathrm{m}}{2}\ln(2\pi) \qquad (3.19)$$

where $\boldsymbol{\theta}$ represents the vector of hyper-parameters in the GPR model. By maximizing the log likelihood with respect to the model parameters (such as the length scale parameter l_q and the variance, we can obtain the optimal parameter values that best fit the observed data and capture the underlying patterns.

Given the training set, i.e. $\mathbf{z}_t$ and $\mathbf{x}_{tk}$ (k = 1, 2, …, m), $\boldsymbol{\theta}$ can be estimated from the maximum likelihood method: [21]

$$\widetilde{\boldsymbol{\theta}} = \underset{\boldsymbol{\theta}}{\operatorname{argmax}}\{\ln\big(L(\boldsymbol{\theta}|\mathbf{z}_t)\big)\} \qquad (3.20)$$

where $\widetilde{\boldsymbol{\theta}}$ is the maximum likelihood estimate of $\boldsymbol{\theta}$. Given $\widetilde{\boldsymbol{\theta}}$, $\mathbf{z}_t$, $\mathbf{x}_{tk}$ and $\mathbf{x}_{ru}$ (u = 1, 2, …, n-m), the updated mean and covariance of $\mathbf{Y}_r$ conditional on $\mathbf{z}_t$ can be readily obtained from Eq. (3.17). The commercial software Matlab R2021a is used to implement the GPR model.

3.4.2 Results

The GPR is set to predict the correction factor to be applied to the PCC-2 model. That is, the correction factors for different cases are assumed to follow a Gaussian process, i.e. $\mathbf{Y}(\mathbf{x})$ in Section 3.4.1. Ideally, this factor should be equal to $P_{PCC\text{-}2}/P_{FEA}$. The accuracy of the GPR model is depicted on Fig. 3.3. The 95% confidence interval, taken as $f_{GPR} \pm 1.96\eta_r$ where η_r is the posterior standard deviation of the correction term for the regression set. The output data from the FEA is depicted in the Figure for comparison. The figure shows that the GPR model successfully predicted the necessary correction factor for almost all of the 259 cases of the regression set.

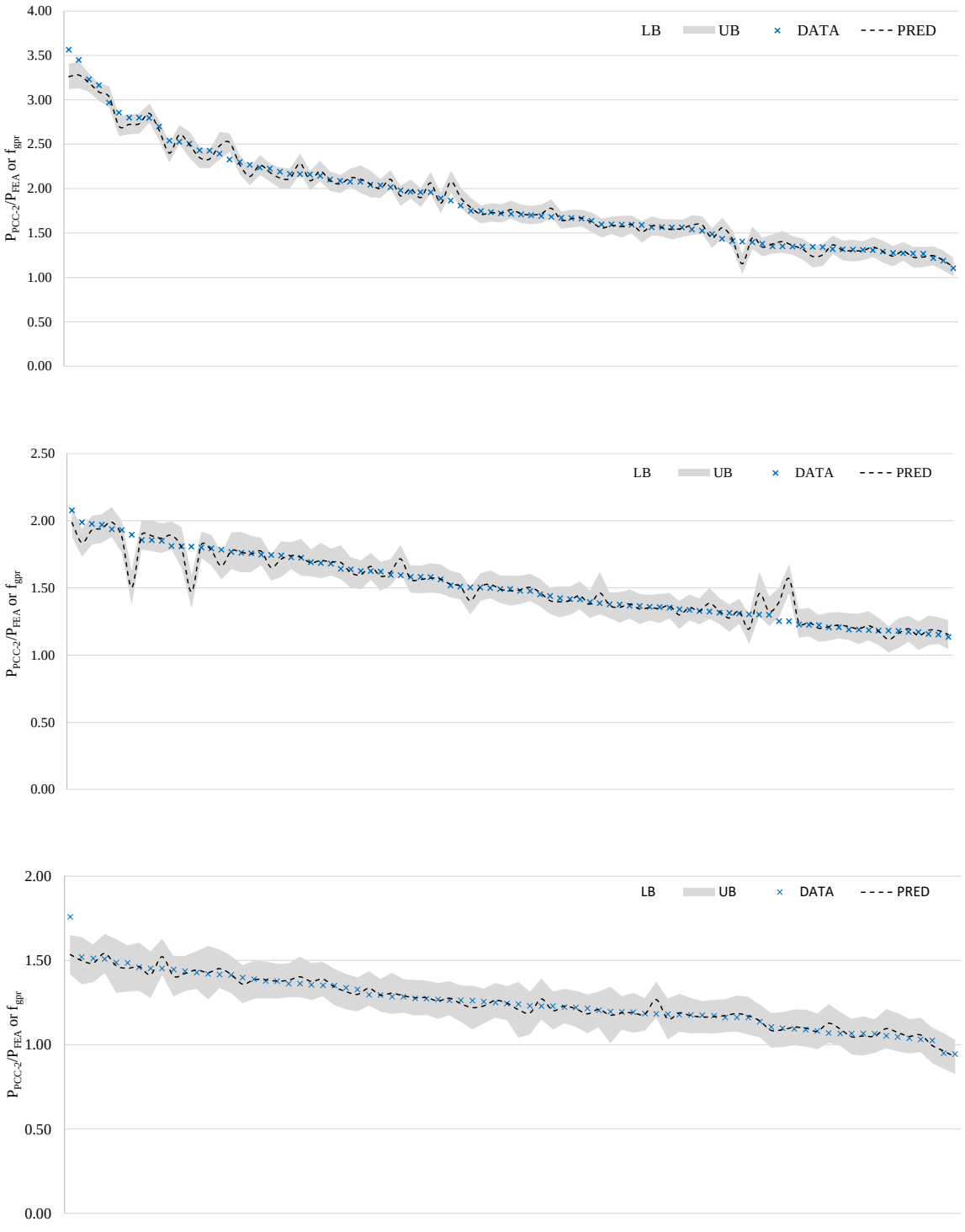

Figure 3.3 95% Confidence interval for the GPR predicted correction factor of the test set

As to the burst capacity predicted by the proposed model P_{GPR}, the results show a significant improvement over the accuracy of the PCC-2 model when compared with P_{FEA}. The mean value and COV of P_{GPR}/P_{FEA} for the testing set are 1.0 and 4.0%, respectively. Table 3.1 and Fig. 3.4 compare the accuracy of the PCC-2 model and proposed GPR model.

Table 3.1 Mean and COV of PCC-2 and the proposed GPR model for the 259 cases (regression set)

	P_{FEA}/P_{PCC-2}	P_{FEA}/P_{GPR}
Mean	1.56	1.00
COV	0.46	0.04

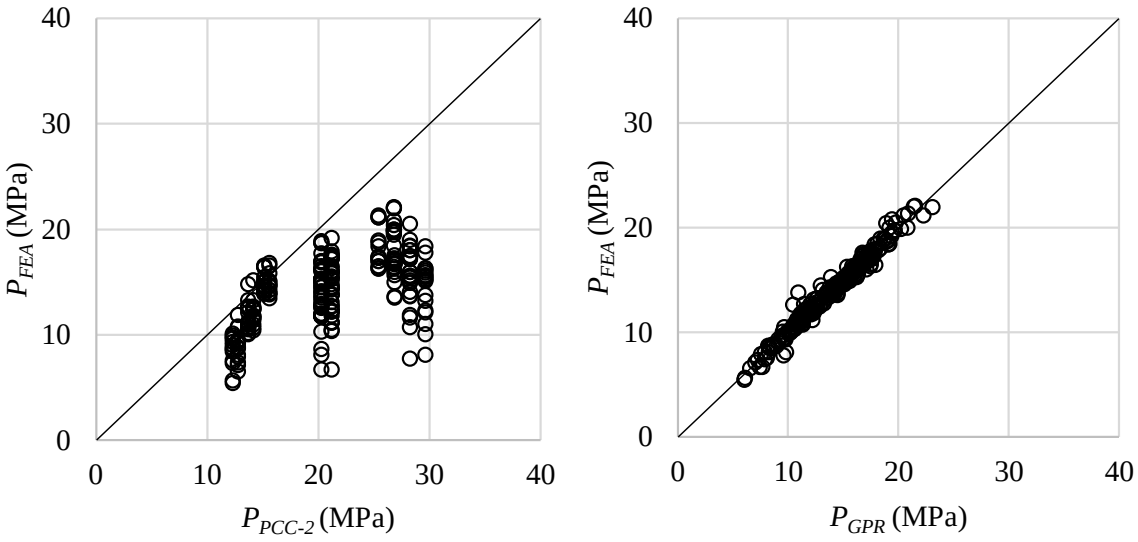

Figure 3.4 Accuracy of the PCC-2 and GPR model

Being on the denominator in the fraction of Eq. (3.17), it follows that the input variable with a higher length scale l_q has less correlation with the output values. Table 3.2 presents the standard deviation and the length scales of the GPR model. It can be observed that the two input variables that have marked effects on the magnitude of the correction factor are the normalized depth of the defect, and elastic modulus of the composite. All the parameters had some correlation to the correction factor predicted, but for the ranges used

on the parametric analysis the transversal tension resistance of the composite and the length of the defect play a minor role compared to other parameters.

Table 3.2 Hyperparameters of the GPR model

Description	Symbol	Max. likelihood estimate	Associated input variable
Std. dev. of *Y*	η_y	1.83	N/A
Std. dev. of noise	η_n	0.05	N/A
Length scales in the SE kernel	l_1	0.40	$\frac{d}{t}$
	l_2	5.54	$\frac{L^2}{Dt}$
	l_3	2.65	$\frac{w^2}{Dt}$
	l_4	2.07	$\frac{th_{repair}}{th_{pcc2}}$
	l_5	0.76	$\frac{E_c}{E}$
	l_6	2.14	$\frac{Y}{T}$
	l_7	8.81	$\frac{Y_T}{X_T}$

3.5 Conclusions

The burst capacity of CRC pipelines is investigated in this study. A parametric analysis of 864 cases was performed to investigate the effect of the defect geometry and the material properties on the accuracy of the ASME PCC-2 model, which is shown to be inaccurate to predict the burst capacity of CRC pipelines with localized defects. To account for the different variables that affect the burst capacity, the Gaussian process regression (GPR) is employed to predict a correction factor to improve the accuracy of the model. This correction factor is assumed to be a function of seven normalized input variables to characterize the defect geometry and the materials properties.

The 864 cases are divided into a training set (70% of the cases) to develop the GPR model and a regression set (30% of the cases) to validate the model accuracy. The correction

factor is shown to be effective and consistent. The mean and COV of the FEA-to-predicted ratios equal 1.00 and 4.0%. The hyperparameters involved in the GPR model indicate that the normalized defect depth and the elastic modulus play a key role in the improvement of the burst capacity model. This study offers new insights into the burst capacity of CRC pipelines, and a viable alternative to improve the accuracy of the burst capacity model derived from the ASME PCC-2 equation.

References

[1] K.S. Lim, S. Azraai, N. Yahaya, M. Noor, N. Yahaya. An Overview of Corroded Pipe Repair Techniques Using Composite Materials. International Journal of Materials and Metallurgic Engineering. 10 (2016) 19-25

[2] M.L. Deng, C. Bao, A.T.S. Hung, N. Md Noor, K.S. Lim. Effect of defect geometries upon burst capacity of composite repaired pipe. Physics and Chemistry of the Earth. 128 (2022) 103274

[3] K.S. Lim, S. Azraai, N. Yahaya, M. Noor, L. Zardasti, JHJ. Kim. Behaviour of steel pipelines with composite repairs analyzed using experimental and numerical approaches. Thin-Walled Struct. 139 (2019) 321–33

[4] International Standard Organization. ISO-24817 Petroleum, petrochemical and natural gas industries: composite repairs for pipework: Qualification and design, installation, testing and inspection (2017)

[5] American Society of Mechanical Engineers. Non Metallic and Bonded Repairs. In ASME PCC-2-2018 Repair of Pressure Equipment and Piping: An American national standard (2018)

[6] J. Duell, J. Wilson, M. Kessler. Analysis of a carbon composite overwrap pipeline repair system. The International journal of Pressure Vessels and Piping 85(11) (2008) 728-788

[7] H. da Costa Mattos, J.M. Reis, M. Da Silva, F. Amorim, V. Perrut. Analysis of a glass fibre reinforced polyurethane composite repair system for corroded pipelines at elevated temperatures. Composite structures 114 (2014) 117-123

[8] P.H. Chan, K.Y. Tshai, M. Johnson, L.H. Choo, S. Li, K. Zakaria. Burst strength of carbon fibre reinforced polyethylene strip pipeline repair system – a numerical and experimental approach. Journal of Composite Materials 49(6) (2015) 749-756

[9] A. Ali, M. Zahiraniza, M. Thar. Burst capacity of pipe under corrosion defects and repaired with thermosetting liner. Steel and composite structures 35(2) (2020) 171-186

[10] J. Chen, H. Wang, M. Salemi, P.N. Balaguru. Finite element analysis of composite repair for damaged steel pipeline. Coatings 11(3) (2021) 301

[11] S. Zhang, W. Zhou. Assessment of effects of idealized defect shape and width on the burst capacity of corroded pipelines. Thin-walled structures 154 (2020) 106806

[12] X.K. Zhu, B.N. Leis. Influence of the yield-to-tensile strength ratio on failure assessment of corroded pipelines. Journal of pressure vessel technology 127(4) (2005) 436-442

[13] Dowling, N. E. (2007) Mechanical behavior of materials : engineering methods for deformation, fracture and fatigue. 3rd ed. Upper Saddle River, NJ: Pearson Prentice Hall.

[14] L. Meniconi, J. Freire, R. Vieira, J. Diniz. Stress analisis of pipelines with composite repairs. Proceedings of the 2002 4th International Pipeline Conference (2002) 2031-2037

[15] Z. Hashin. Failure criterion for unidirectional fiber composites. Journal of applied mechanics 47(2) (1980) 329-334

[16] R. Her, J. Renard, V. Gaffard, Y. Favry, P. Wiet. Design of pipeline composite repairs: from lab scale tests to FEA and full-scale testing. Proceedings of the 2014 10th international pipeline conference Vol.2 (2014)

[17] L. Mazurkiewicz, M. Tomaszewski, J. Malachowski, K. Sybilski, M. Chebakov, M. Dimitrenko. Experimental and numerical study of steel pipe with part-wall defect reinforced with fibre glass sleeve. The International Journal of Pressure Vessels and Piping 149 (2017) 108-119

[18] S. Ahankari, A. Patil. Sea water effect on mechanical performance of steel pipes rehabilitated with glass fiber reinforced epoxy composites. Materials today: Proceedings 22 (2020) 2490-2498

[19] D. Kong, X. Huang, M. Xin, G. Xian. Effects of defect dimensions and putty properties on the burst performances of steel pipes wrapped with CFRP composites. The International Journal of Pressure Vessels and Piping 186 (2020) 104-139

[20] R.T. Ferreira, I.A. Ashcroft. Optimal orientation of fiber composites for strength based on Hashin's criteria optimality conditions. Structural and multidisciplinary optimization 61(5) (2020) 2155-2176

[21] He, Z. & Zhou, W. Improvement of burst capacity model for pipelines containing dent-gouges using Gaussian process regression. Engineering structures. 272 (2022).

[22] Bishop, C. M. (2006). Pattern recognition and machine learning. Springer.

[23] Rasmussen, C. E., & Williams, C. K. I. (2019). Gaussian processes for machine learning. The MIT Press.

[24] Do, C.B. Gaussian Processes. Scholarpedia, 7(10) (2012) 1623

[25] Pilario, K. E. et al. A Review of Kernel Methods for Feature Extraction in Nonlinear Process Monitoring. Processes. 8,24 (2020).

Chapter 4

4 Conclusions and Recommendations for future study

4.1 General

The core contributions of the present thesis are:

- Demonstrate the defect width effect on the burst capacity of CRC pipelines
- Explain mechanistically why CRC pipelines with localized defects have lower burst capacities than full/circumferential ones
- Propose an improvement to the existing ASME model to incorporate these two effects
- Evaluate the parameters that play an important role in the burst capacity calculation and that are not being currently considered on existing models
- Propose a model that can be used to rapidly calculate the burst capacity of CRC pipelines with adequate accuracy.

4.2 Investigation of the defect depth on the burst capacity of composite-repaired pipelines with corrosion defects using finite element analysis

In chapter 2, an FEA was conducted to investigate the effect of the corrosion defect width on the burst capacity of CRC pipelines. The finite element model was validated using full-scale burst tests of CRC pipe specimens reported in the literature. The analysis results indicated that the burst capacity of a CRC pipeline with a localized corrosion defect was markedly lower than that of a CRC pipeline with a full-circumferential defect of the same depth and length. The reduction in burst capacity was found to be greater for deeper defects. This reduction was attributed to the significant bulging response observed under internal pressure for pipelines containing localized corrosion defects.

Furthermore, it was observed that the burst capacity model derived from the design equation recommended in the ASME PCC-2 code was markedly non-conservative for CRC pipelines containing localized corrosion defects when compared with the results from the parametric FEA. To address this issue, an empirical equation for the defect width correction factor was developed through non-linear regression analyses. This correction factor was then applied to the prediction made by the PCC-2 model. The application of the width correction factor significantly improved the predictive accuracy of the PCC-2 model for CRC pipelines with localized corrosion defects. This study emphasizes the importance of considering the defect width when evaluating the burst capacity of such pipelines, and the corrected PCC-2 model provides a more reliable prediction method in these cases.

4.3 Development of an enhanced model to predict the burst capacity of composite repaired corroded pipelines using Gaussian process regression

Chapter 3 investigates the burst capacity of CRC pipelines by conducting a parametric analysis of 864 cases. The analysis focuses on examining the influence of defect geometry and material properties on the accuracy of the ASME PCC-2 model, which has been found to be inaccurate in predicting the burst capacity of CRC pipelines with localized defects.

To address the various factors affecting burst capacity, Gaussian process regression (GPR) is employed to predict a correction factor that enhances the accuracy of the model. This correction factor is assumed to be a function of seven normalized input variables, which characterize the defect geometry and material properties. The 864 cases are divided into a training set (70% of the cases) used to develop the GPR model and a regression set (30% of the cases) employed to validate the model's accuracy. The correction factor is demonstrated to be effective and consistent, with a mean FEA-to-predicted ratio of 1.00 and a coefficient of variation (COV) of 4.0%.

The hyperparameters associated with the GPR model indicate that the normalized defect depth and elastic modulus play a crucial role in improving the burst capacity model. These findings offer new insights into the burst capacity of CRC pipelines and provide a viable

alternative to enhance the accuracy of the burst capacity model derived from the ASME PCC-2 equation.

4.4 Recommendations for future study

The recommendations to continue this research topic are summarized as follows:

1. The magnitude of the effect of the defect width is related to material properties such as the elastic modulus of the composite. Further research including modern materials like carbon fibre with high elastic modulus should be investigated to assess the effect in such cases.

2. The research focuses on uni-directional fibers only. The failure on the transversal direction (i.e. failure mode MTCRT) could be assessed considering a multidirectional fibre to establish a power-law and include enough reinforcement in the transverse direction to force failure to happen on the circumferential direction.

Curriculum Vitae

Name:	Rodrigo Silva Silva-Santisteban
Post-secondary Education and Degrees:	Universidad Peruana de Ciencias Aplicadas Lima, Peru 2011-2017 B.A.
	The University of Western Ontario London, Ontario, Canada 2021-2023 MESc
Related Work Experience	Specialized Engineer (FRP pipes design) Sarplast Peru 2017-2021
	Teaching Assistant The University of Western Ontario 2022-2023